Enhancing Performance of Biocarriers Facilitated Gravity-Driven Membrane (GDM) Reactor for Decentralized Wastewater Treatment: Effect of Internal Recirculation and Membrane Packing Density

Seonki Lee [a,b], Guillaume Olivier Badoux [c,d], Bing Wu [a,e,*], Tzyy Haur Chong [a,b,**]

[a] Singapore Membrane Technology Centre, Nanyang Environment and Water Research Institute, Nanyang Technological University, 1 Cleantech Loop, Clean Tech One 06-08, Singapore 637141

[b] School of Civil and Environmental Engineering, Nanyang Technological University, 50 Nanyang Avenue, Singapore 639798

[c] Eawag, Swiss Federal Institute of Aquatic Science and Technology, 8600, Dübendorf, Switzerland

[d] ETH Zürich, Institute of Environmental Engineering, 8093, Zürich, Switzerland

[e] Faculty of Civil and Environmental Engineering, University of Iceland, Hjardarhagi 2-6, IS-107 Reykjavik, Iceland

*Corresponding author: E-mail: wubing@hi.is

**Corresponding author: E-mail: THChong@ntu.edu.sg

Abstract

This study aims to investigate the effect of internal recirculation and membrane packing density on the performance (water quality, membrane performance, and microbial community) of a biocarriers facilitated gravity-driven membrane (GDM) reactor under intermittent aeration condition. The results revealed that the presence of internal recirculation in the GDM reactors could effectively improve water quality (especially increasing nitrogen removal) and membrane performance (especially reducing cake layer resistance) compared to those without internal recirculation. In addition, compared to a high packing density membrane module (1150 m^2/m^3), a lower packing density membrane module (290 m^2/m^3) benefited to improve 15% of nitrogen removal and 44% of permeate flux due to the effective aeration scouring effect and less-limited eukaryotic activity, as well as reduce 20% of total treatment cost. In addition, the presence and absence of internal recirculation could lead to dissimilar microbial community compositions of the biofilms in the GAC layers and on the membrane surfaces. However, the membrane packing density could play an insignificant effect on the microbial community compositions of the biofilms in the GDM reactors with internal recirculation.

Keywords: Decentralized wastewater treatment; Gravity-driven membrane; Recirculation; Membrane packing density; Nitrogen removal

1. Introduction

Decentralized wastewater treatment systems have been considered as an adoptable option in rural areas and developing countries due to their inexpensive installation, easy operation, and low operating and maintaining cost. Traditional decentralized systems, such as constructed wetland and septic tank, have been well applied in treating wastewater, however, nowadays they are facing challenges due to their limit in meeting the increasingly strict discharge standards (Nguyen et al. 2007).

Recently, gravity-driven membrane (GDM) reactors have been developed as an alternative decentralized system in treating greywater/municipal wastewater (Ding et al. 2016, Ding et al. 2017, Jabornig and Podmirseg 2015, Künzle et al. 2015, Lee et al. 2019, Wang et al. 2017). The GDM reactor is a membrane-based process driven by natural hydrostatic gravity force, therefore, it can produce superior permeate water without requiring permeate suction pump and membrane chemical cleaning protocols. This guarantees that the GDM can be operated with significantly lower energy consumption and capital cost than conventional membrane bioreactors. It has been well illustrated that the stabilized permeate flux achieved in the GDM reactor was attributed to the heterogeneous biofilm layer formed on the membrane surface, in which organic degradation, prokaryotes proliferation, and eukaryotes movement/predation occurred and their contributions to the biofilm formation displayed a relatively steady pattern (Peter-Varbanets et al. 2010, Tang et al. 2018).

However, GDM reactors had relatively lower permeate fluxes (<10 $L/m^2/h$) in treating wastewater due to lower driving force and limited biodegradation of organics. To further improve permeate flux, integrating GDM reactors with aeration, coagulation, and biocarriers have been well documented (Ding et al. 2017, Jabornig and Podmirseg 2015, Künzle et al. 2015, Lee et al. 2019). In a previous study (Lee et al. 2019), we developed a hybrid upflow

packed-bed granular activated carbon (GAC) facilitated GDM reactor and operated it at an intermittent aeration mode (aeration diffuser was located above the GAC bed). The results showed that this combination could effectively improve membrane performance as well as the organic (87.8-90.5%) and nitrogen removal (29.3-37.1%) compared to the GDM reactor without intermittent aeration. It was also found that intermittent aeration could negatively influence the nitrogen removal efficiency because (1) a high level (~3.5 mg/L) of residual dissolved oxygen (DO) in the membrane zone during non-aeration period resulted in poor denitrification of the biofilm attached on the membrane; and (2) the anoxic biofilm on the GAC carriers had limited contribution to denitrification due to less available nitrite/nitrate. Thus, to maximize nutrient removal in the GAC+GDM reactors, installation of internal recirculation in the reactor could be considered, aiming to deliver nitrite/nitrate-contained effluent in the intermittent aeration zone to the anoxic GAC zone and enhance denitrification of the biofilm on the GAC carriers. Meanwhile, it has been reported that sponge modified plastic carriers facilitated immobilizing more microorganisms due to their high porosity nature and improving organic and nutrient removals in moving bed biofilm reactor systems (Deng et al. 2016).

In addition, compared to MBRs, the GAC+GDM reactors had lower permeate fluxes. Therefore, a GAC+GDM reactor requires more membrane area with a higher membrane packing density than a conventional submerged MBR under the same water productivity and footprint scenarios. It has been reported that the high packing density of membrane module in MBRs suffered more serious fouling due to ineffective air scouring (Braak et al. 2011). The non-aeration GDM systems with high packing density hollow fibre membrane modules also had lower permeate fluxes in pre-treating seawater, possibly because of limited predation and movement behaviors of eukaryotes between the insufficient space of hollow fibres (Wu et al. 2017). Furthermore, the membrane packing density (i.e., membrane area) determined hydraulic retention time (HRT)

of the GDM reactors, which was also associated with water quality (Wu et al. 2019). Thus, it is necessarily important to optimize the membrane module density in the GAC+GDM reactors in order to maximize wastewater treatment capability with reduced footprint.

In this study, internal recirculation and moving biocarriers were introduced to the biocarriers facilitated GDM system in treating municipal wastewater to enhance the reactor performance (nutrient removal and permeate flux). In addition, the effect of membrane packing density on water quality, membrane performance, microbial community, and cost were examined.

2. Materials and methods

2.1. Setup and operating conditions of biocarriers facilitated GDM reactors

Two laboratory-scale biocarriers facilitated GDM reactors (working volume of 8.6 L) with internal recirculation were operated in parallel. As shown in Figure 1, the GAC biocarriers (1.25 kg; Filtrasorb 300, US) were placed on the bottom of the reactor, and the Kaldnes K3 plastic biocarriers (120 pcs; China) that were modified by inserting a sponge cube (10 mm × 10 mm, Aquaporous Gel, Japan) into a plastic biocarrier's void space were floated on the top of the reactor (Deng et al. 2016). Two identical hollow fiber membrane modules (PVDF; 150 kDa) were installed at ~30 cm below the water level (i.e., a hydrostatic pressure of ~30 mbar). An air diffuser was located between the GAC layer and the membrane modules. Intermittent aeration (30 min aeration at 0.5 L/min followed by 60 min non-aeration) was delivered into the GDM reactor by using a timer-controlled aeration pump (Lee et al. 2019). The feed wastewater was introduced from the feed tank to the bottom of the reactor by a peristaltic pump and its flow rate was manually adjusted according to the permeate flow rate in order to minimize the overflow. The mixed liquor at the top of the reactor was recirculated back to the bottom of the reactor using a peristaltic pump with a constant flow rate (0.52 L/h).

In one reactor (hereinafter R1-HP), two membrane modules with the high membrane packing density (1150 m^2/m^3; membrane area of 268 cm^2 per module) were installed, while in the other reactor (hereinafter R2-LP), two membrane modules with the low packing density (290 m^2/m^3; membrane area of 69 cm^2 per module) were employed (Table 1). The feed wastewater was collected from the primary clarifier in the Ulu Pandan Wastewater Reclamation Plant in Singapore. There was no sludge discharge and membrane cleaning during the whole period of operation. The room temperature was kept at 20°C.

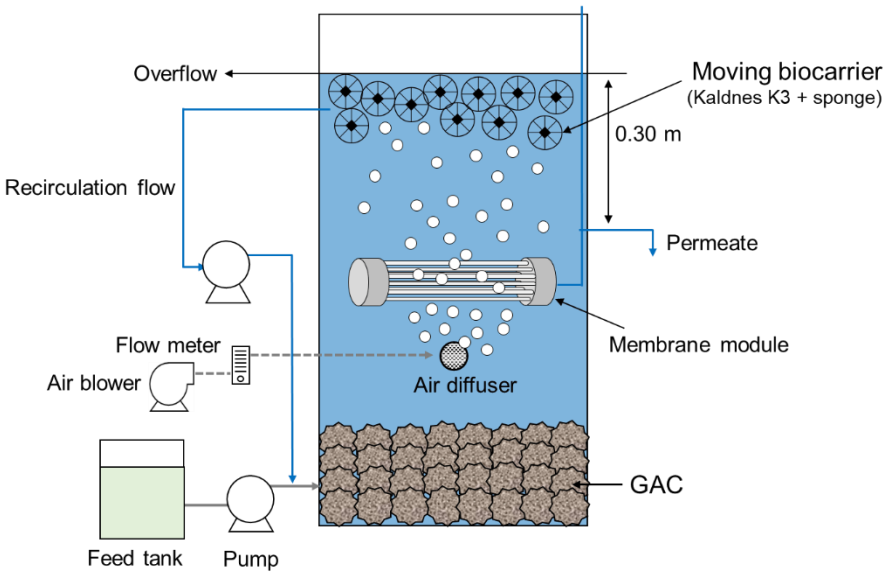

Figure 1. A schematic diagram of the biocarriers facilitated GDM reactor.

Table 1. Operating conditions of the biocarriers facilitated GDM reactors.

	R1-HP	R2-LP
pH	7.3±0.4	7.2±0.2
DO (mg/L)	3.4±0.7	3.8±0.9
Effective total membrane area (cm^2)	536	138
Membrane packing density (m^2/m^3)	1150	290
Averaged HRT[a] (h)	~59	~154
Averaged recirculation ratio[b]	~3.5	~9.2

[a] HRT was determined daily and averaged HRT was calculated by averaging the daily HRT.
[b] The recirculation ratio was defined as the ratio of recirculation flow rate (0.52 L/h) to the feed flow rate. Averaged recirculation ratio was calculated by averaging the daily recirculation ratio.

2.2. Water quality analysis

The feed, reactor, and permeate samples were periodically collected and then filtered with 0.45 μm syringe membranes (Millipore, USA) and filtrate was kept at 4℃ before analysis. The dissolved organic carbon (DOC) and total nitrogen (TN) were determined using a TOC/TN analyzer (TOC-VCSH/TNM-1, Shimadzu, Japan). Soluble organic fractions in the water samples were determined by an LC-OCD analyzer (LC-OCD Model 8, DOC-LABOR, Germany), a size-exclusion chromatography coupled with organic carbon detector and organic nitrogen detector. According to the molecular weight, the organic fractions were classified into five groups, i.e., biopolymers (MW > 20 kDa), humic substances (MW ~1000 Da), building blocks (MW ~300-500 Da), low molecular weight (LMW) acids and neutrals (MW < 350 Da). The details in operation and analysis procedures were referred from the literature (Huber et al. 2011).

Ammonia (NH_4-N), nitrite (NO_2-N), and nitrate (NO_3-N) were measured using the spectrometric method with Ammonia TNT 830, 831, 832 kit (Hach, USA), Nitrite LCK 341 kit (Hach Lange GmbH, Germany), and Nitrate TNT 835 kit (Hach, USA), respectively. The pH and dissolved oxygen (DO) were periodically monitored using a portable pH meter (Mettler Toledo, Switzerland) and a portable DO meter (Mettler Toledo, Switzerland), respectively.

To illustrate the statistical significance, a two-sample t-test was conducted by comparing the sampling data groups under two different conditions. The p-values for the two-sample t-test were calculated at a significance level of 0.05.

2.3. Fouling resistance

To characterize the membrane fouling, the fouling resistance was evaluated based on the resistance-in-series model (Broeckmann et al. 2006). At the end of experiment (the total resistance R_t was calculated based on the final permeate flux), the membrane module was

147 removed from the reactor, and cake layer was physically detached by rinsing with Milli-Q
148 water for 10 min and followed by sonication for 15 min. Then, the permeate flux of the
149 physically-cleaned membrane was measured at the hydrostatic pressure of 30 mbar and the
150 resistance was calculated as $(R_m + R_{ir})$. The biofilm cake resistance (R_c) was obtained by
151 subtracting the resistance after physical cleaning $(R_m + R_{ir})$ from the total resistance (R_t). In
152 addition, the irreversible fouling resistance (R_{ir}) was achieved by subtracting the intrinsic
153 membrane resistance (R_m) from the resistance after physical cleaning $(R_m + R_{ir})$.

154 **2.4. Microbial community**

155 At the end of experiment, biofilms were collected from the membrane module, GAC biocarriers,
156 moving biocarriers (i.e. Kaldnes K3 with sponge), and then kept at -20℃ before DNA
157 extraction. Genomic DNA was extracted from biofilms using PowerSoil® DNA isolation kit
158 (MO bio, USA). The prokaryotic and eukaryotic microbial communities in biofilms were
159 analyzed using the 16S and 18S rRNA sequencing, respectively, on the Illumina MiSeq
160 platform. Primers 357wF (CCTACGGGGNGGCWGCAG) and 785R
161 (GACTACHVGGGTATCTAATCC) for prokaryotes, TAReukF
162 (CCAGCASCYGCGGTAATTCC) and TAReukR (ACTTTCGTTCTTGATYRA) eukaryotes
163 were chosen. The sequencing results were analyzed by the standard de novo operational
164 taxonomic unit (OTU)-based approach using QIIME software (Caporaso et al. 2010).

165 **3. Results and Discussion**

166 **3.1. Effect of membrane packing density**

167 3.1.1. Organic removal

168 Both GDM reactors were operated in parallel for 45 days. As the feed water flow was daily

regulated based on the permeate flow (i.e., minimizing overflow), within 45-day operation, R1-HP and R2-LP achieved dissimilar HRTs and internal recirculation ratios due to different membrane packing densities (i.e., membrane areas) (Table 1). Increasing membrane packing density led to a decreased HRT (~59 h for R1-HP *vs.* ~154 h for R2-LP) and internal recirculation ratio (~3.5 for R1-HP *vs.* ~9.2 for R2-LP). However, both HRT and internal recirculation ratio parameters did not impact pH and DO levels in the reactors.

Figure 2 shows the DOC concentrations in the feed, reactor and permeate. The DOC in the feed ranged ~24-53 mg/L (averaged at 39.0 mg/L) throughout the whole period of experiment. During the early stage (from Day 0-20), the DOC level in the R1-HP (~6.3-10.7 mg DOC/L) was higher than that of R2-LP (~3.3-6.8 mg DOC/L). This indicated that the shorter HRT and lower recirculation ratio of R1-HP could result in slightly lower organic removal efficiency during the early stage (~79.0% for R1-HP *vs.* ~88.1% for R2-LP; $p<0.05$), possibly associating with the suppressed biodegradation capacity under higher organic loading (shorter HRT). However, the DOC levels in R1-HP decreased with extending operation time (~3.4-6.3 mg/L), showing gradually enhanced biodegradation efficiency. In addition, LC-OCD analysis revealed that with extending operation time, the removal efficiency of biopolymers in R1-HP increased from ~16% (Day 0-20) to ~58% (Day 21-45), while those of humic substances, building blocks, LMW neutrals, and LMW acids were relatively constant (Figure 3). This illustrated that the improved biodegradation of biopolymers contributed to the increasing organic removal efficiency. After both reactors reached the stable stage, they achieved the comparable biodegradable DOC removal ratio (~88.5% for R1-HP *vs.* ~91.4% for R2-LP; $p>0.05$).

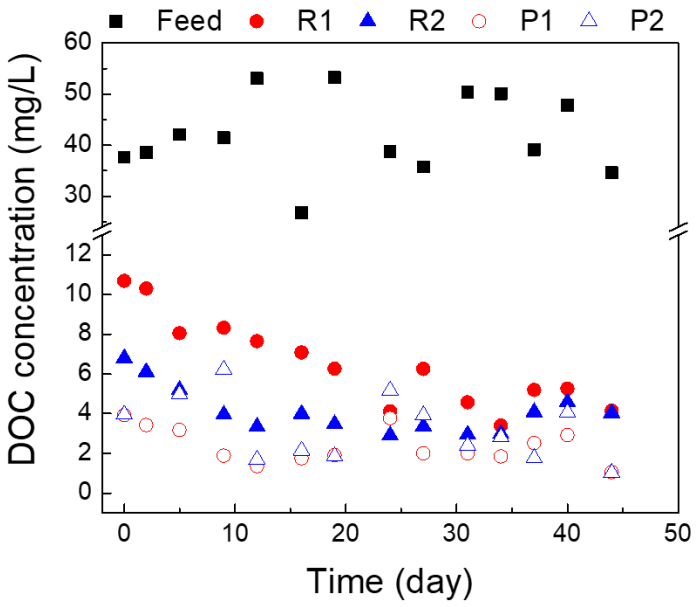

Figure 2. DOC concentrations in the feed, reactor, permeate of R1-HP and R2-LP. R and P represent reactor and permeate, respectively.

In addition, in both GDM reactors, the DOC levels in the permeates (~2.3-3.0 mg DOC/L) were only slightly lower than those in the reactors (~3.6-4.7 mg DOC/L, Figure 2), which suggested that membrane separation contributed only ~1-6% of the overall DOC removal. As shown in the Figure 3, the biopolymers in the permeate were much less than those in the reactors, showing that part of biopolymers could be effectively retained by the membrane. On the other hand, the concentrations of small-sized organics, such as humic substances, building blocks, and LMW acids, were relatively comparable in the reactor and in the permeate. In addition, LMW neutrals concentrations in the permeates were higher than those in the reactors. Possibly, the greater-sized organic matters on the membrane were hydrolyzed or biodegraded (by the biofilm) to small-sized soluble organic molecules, which could pass through the membrane and presented in the permeate. Similar findings were also observed in the previous GDM studies (Lee et al. 2019, Pronk et al. 2019). Nevertheless, both reactors achieved comparable organic levels in the permeate (2.3±0.9 mg/L for R1-HP and 3.0±1.4 mg/L for R2-LP; $p>0.05$).

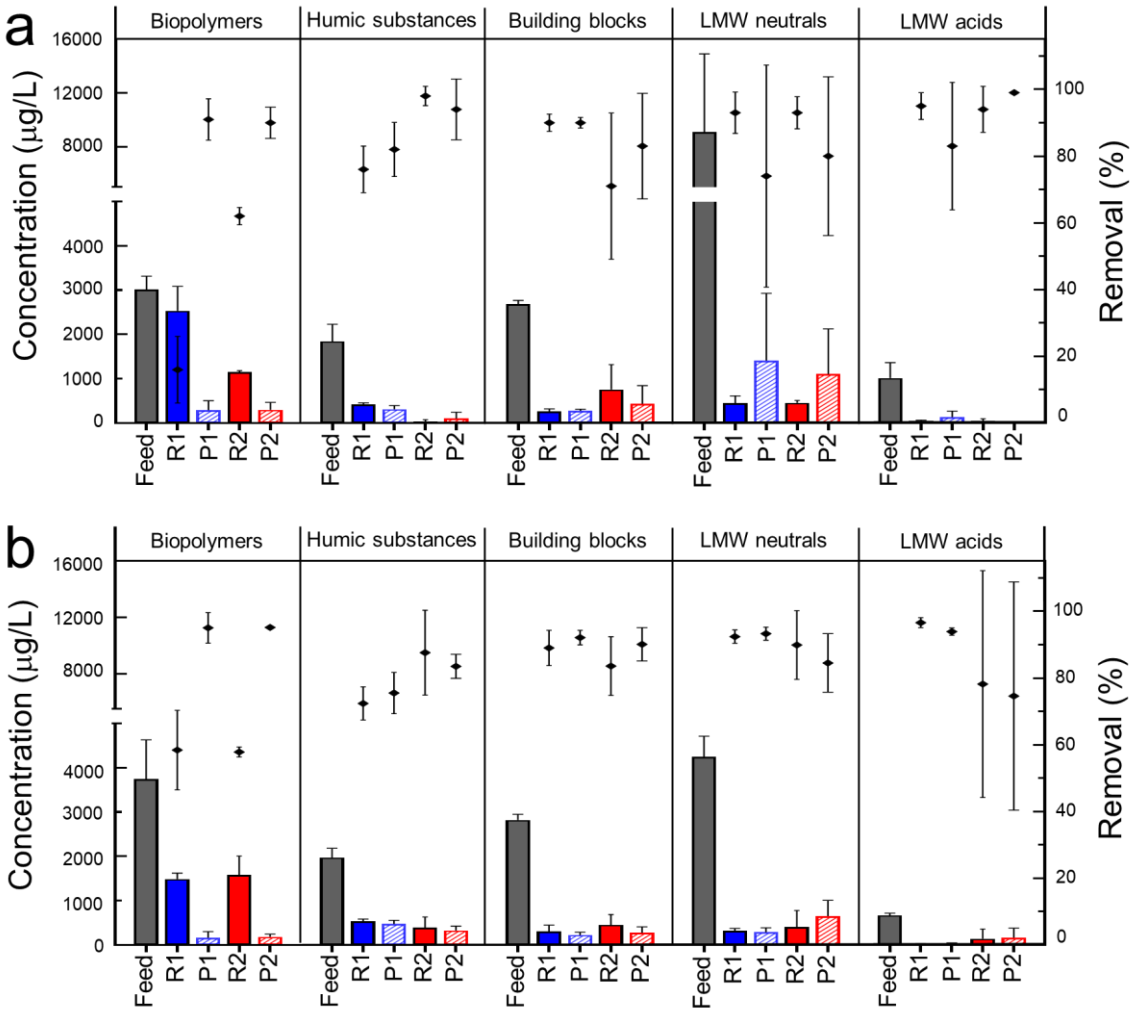

Figure 3. Soluble organic fractions in the feed, reactor, and permeate of R1-HP and R2-LP. (a) during initial stage (Day 0-20, n=2), and (b) during stable stage (Day 21-45, n=3). Columns indicate the concentrations while dots indicate the removal efficiency calculated based on the data in the feed. R and P represent reactor and permeate, respectively.

3.1.2. Nitrogen removal

Figure 4 shows the nitrogen concentrations in feed, reactor, and permeate in both reactors. At the initial period (Day 0-9), total nitrogen (TN) was not effectively removed in both reactors due to poor nitrification (Figures 4a and b). However, during Day 9-12, the performance of nitrification process was remarkably improved, in which the ammonia was mainly converted to nitrite (up to ~7 mg NO_2-N/L, Figure 4c) instead of nitrate (Figure 4d). Afterwards, only very limited ammonia were detected in both reactors (~1.2±0.5 mg NH_4-N/L for R1-HP and

~0.8±0.2 mg NH_4-N/L for R2-LP), showing complete nitrification in both reactors. Meanwhile, the concentration of nitrite in the reactors decreased gradually, which was converted to nitrate. The temporary nitrite accumulation phenomenon during the initial period can be speculated that the activity of nitrite-oxidizing bacteria (NOB) might be lower than that of ammonia-oxidizing bacteria (AOB). It has been well documented that compared to AOB, NOB was often more susceptible to environmental stress such as an acute concentration or loading of free ammonia (Alleman 1985, Rhee et al. 1997). With extending operation time, the NOB activity was enhanced attributed by the decreased ammonia concentration.

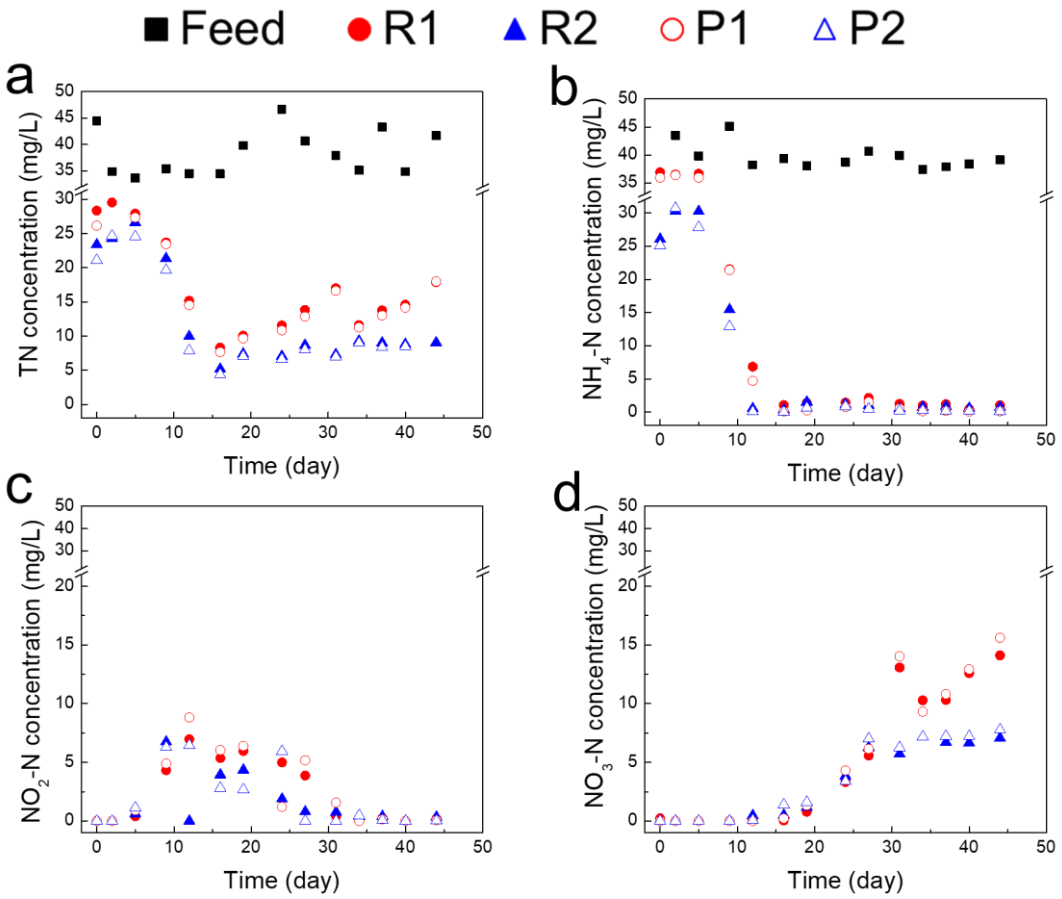

Figure 4. Nitrogen concentrations in the feed, reactor, permeate of R1-HP and R2-LP. (a) TN, (b) Ammonia, (c) Nitrite, (d) Nitrate. R and P represent reactor and permeate, respectively.

Obviously, after Day 20, both reactors had dissimilar concentrations of nitrate and total nitrogen. The lower concentrations of nitrate and total nitrogen were found in R2-LP (~6.2 mg NO_3-N/L and ~8.5 mg TN/L) than those in R1-HP (~9.9 mg NO_3-N/L and ~14.3 mg TN/L). Accordingly, the denitrification ratio of R2-LP (~81.9%) was greater than that of R1-HP (~69.0%), which was associated with the longer HRTs and higher recirculation ratio in R2-LP than R1-HP. As a result, R2-LP achieved the higher biological TN removal efficiency (~78.6%) compared to R1-HP (~63.8%).

In addition, in both reactors, the ammonia and nitrogen concentrations in the permeate were slightly lower than those in the reactor (p<0.05; paired t-test). However, it contributed only about 1-2% of overall ammonia and nitrogen removal performances of the system. It was probably associated with the limited biomass attached on the membrane because of its periodical removal by intermittent aeration.

3.1.3. Membrane performance

Figure 5a shows the permeate fluxes of R1-HP and R2-LP throughout the operation period. The fluxes of both reactors dropped rapidly for the initial 3 days and then followed a slowly-decreased pattern before reaching relatively constant levels. During Day 30-45, the averaged flux of R2-LP was ~4.5 LMH, which was approximately 44% higher than that of R1-HP (~3.1 LMH). This implies that increasing membrane packing density could lead to a decreased permeate flux under intermittent aeration condition. This was consistent with our previous observation for the GDM reactors (hollow fibre modules) in pre-treating seawater under non-aeration condition (Wu et al. 2017). In addition, the water permeability in this study (~103-150 LMH/bar) were slightly higher than those in the reported GDM systems in treating municipal wastewater (~44-118 LMH/bar, Table S1) (Ding et al. 2017, Lee et al. 2019, Peter-Varbanets et al. 2010, Wang et al. 2017).

To explore the membrane fouling mechanism, the membrane resistance, irreversible fouling resistance, and biofilm cake layer resistance were evaluated. As shown in Figure 5b, both reactors had comparable irreversible fouling resistances (1.55×10^{11} m^{-1} for R1-HP and 1.34×10^{11} m^{-1} for R2-LP), while the biofilm cake layer resistance of R2-LP (0.94×10^{11} m^{-1}) was 46% lower than that of R1-HP (1.72×10^{11} m^{-1}). Thus, the lesser biofilm layer resistance of R2-LP resulted in the higher permeate flux. It was probably attributed to three facts: (1) the lower membrane packing density of R2-LP, i.e., having a larger spacing between membrane fibers (Figure S1), which could be more effective in biofilm detachment by the shear stress generated from aeration and thus less effective membrane filtration area was lost (Braak et al. 2011); (2) the lower membrane packing density could also provide sufficient space for eukaryotic predation and movement activities, benefiting to form more heterogeneous cake layer (the confocal laser scanning microscopy images shown in Figure S2) (Derlon et al. 2013, Klein et al. 2016, Wu et al. 2017); (3) the lower DOC levels in R2-LP during the early period (Figure 2) may result in less formation of the organic condition layer, and thereby less biofouling potential in the following stage (Characklis 1981, Seidel and Elimelech 2002).

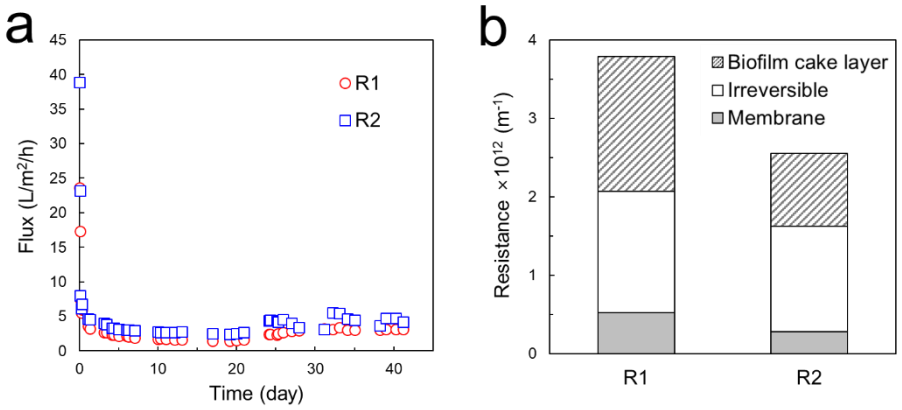

Figure 5. Membrane performances of R1-HP and R2-LP. (a) Permeate flux. (b) Resistance distribution.

3.1.4. Microbial community composition

Figure 6 shows the compositions of prokaryotic and eukaryotic communities in the biofilms derived from GAC particles, moving biocarriers (Kaldnes K3 with sponge), and filtration membranes. In both reactors, Planctomycetes (22.0-47.1%), Proteobacteria (14.2-42.3%), and Verrucomicrobia (12.3-27.3%) were found as major dominant prokaryotic phyla in all biofilms (Figure 6a). In addition, Bacteroidetes and NKB 19, minor dominant phyla, accounted for 1.8-8.4% and 1.4-8.9% respectively, were also detected in all biofilms. These results indicated that the compositions of prokaryotic communities in the biofilms on the GAC, moving biocarriers, and membrane were similar, regardless of membrane packing density.

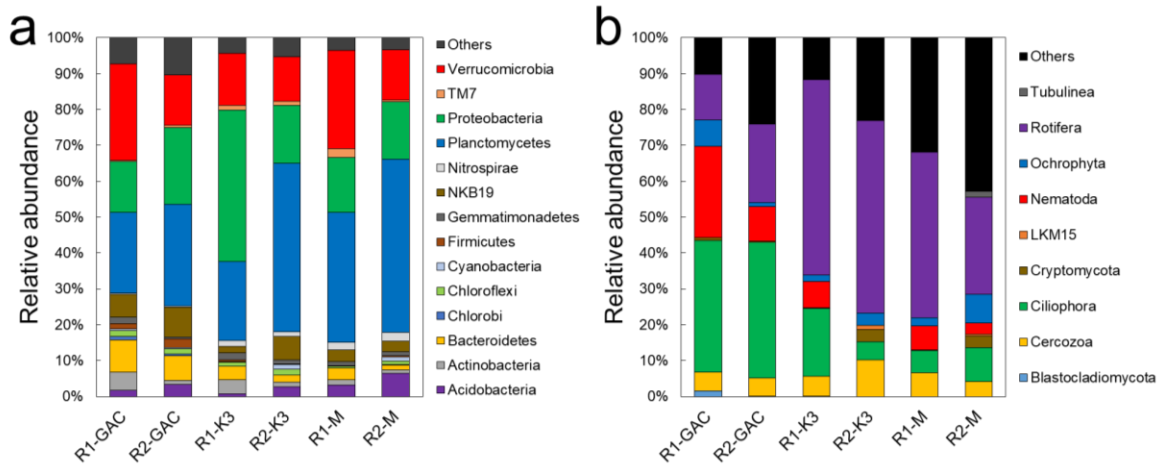

Figure 6. Compositions of prokaryotic (a) and eukaryotic (b) communities in R1-HP and R2-LP. K3 and M represent moving biocarrier (Kaldnes K3 with sponge) and membrane sample, respectively.

As shown in Figure 6b, Rotifera, Ciliophora, Nematoda, and Cercozoa were detected as major eukaryotes in most samples, indicating that the operation conditions (HRT and internal recirculation ratio attributed by membrane packing density) did not influence the predominant compositions of eukaryotic community. However, the abundances of major eukaryotes in the GAC samples were slightly different from those in the moving biocarriers and on the membrane surfaces. In detail, the relative abundances of Ciliophora and Nematoda were much higher in the GAC particles (36.6-37.8% and 9.7-25.4% respectively) than in the moving

biocarriers (5.1-18.8% and ~0-7.4% respectively) and on the membrane surfaces (6.3-9.6% and 3.1-6.7% respectively). In contrast, Rotifera was predominant in the biofilms formed in the moving biocarriers (53.6-54.5%) and on the membrane surfaces (27.1-46.2%), while it was relatively less in the GAC particles (12.7-21.9%). These differences may be derived from the facts that (1) Ciliophora and Nematoda having larger sizes could be trapped within the well-packed GAC layers during recirculation, promoting their accumulations in the GAC particles; and (2) Rotifer may prefer to grow at a relatively higher DO level in the intermittent aeration zone. Nevertheless, the differences in HRTs and internal recirculation ratios caused by different membrane packing densities did not significantly affect the compositions of both prokaryotic community and eukaryotic community.

3.1.5. Energy consumption and water production cost estimation

In this study, the low membrane packing density in the GDM reactor benefited to achieve better membrane performance and improved permeate quality, however it also led to lower water productivity (i.e., wastewater treatment capacity) compared to the high membrane packing density scenario under the same reactor footprint (Table 2). To make a fair comparison, the energy consumption and capital cost of the GDM reactors under different membrane packing density conditions were evaluated and presented in Table 2.

In the energy consumption category, only pump energy and aeration energy were assessed using Eq. (1) and Eq. (2) respectively because the GDM reactors operated without sludge discharge and chemical cleaning in this study.

$$E_{pump} = \frac{\rho g h}{\eta} \frac{Q_{pump}}{Q_p} \qquad (1)$$

$$E_{air} = \frac{\varepsilon Q_{air}}{Q_p} \qquad (2)$$

Where ρ is the density of wastewater (assuming 1000 kg/m^3); g is the gravitational acceleration (9.81 m/s^2); h is the height of water level (0.65 m, i.e., the height between feed pump inlet and water level); η is the pump efficiency (assuming 0.6); ε is the electricity consumption per unit volume of air (assuming 0.019 kWh/m^3 of air) (Maere et al. 2011); Q_{pump} is the flow rate of feed pump or recirculation pump (m^3/s); Q_{air} is the average air flow rate (m^3/s); Q_p is the stabilized permeate flow rate (m^3/s).

The capital cost accounted for reactor construction, pumps, blowers, biocarriers and membranes. The hollow fibre membrane module footprint (1.6-6.2 m^2 membrane area/ m^3 reactor volume) applied in this study were extremely lower than conventional MBRs (<450 m^2/m^3) (Peinemann and Nunes 2010). Therefore, for better estimation of energy consumption and capital cost, it was assumed that 30% of the reactor volume was packed with each membrane module (i.e., 345 m^2 membrane area/m^3 reactor volume in R1-HP and 87 m^2/m^3 in R2-LP). In addition, the average recirculation ratio (3.5 for R1-HP and 9.2 for R2-LP) was used in the estimation of recirculation energy and cost

It is important to recall that in this study, energy input (recirculation and aeration) and footprint (reactor, biocarriers, and other equipment) were identical in both reactors, and the only difference was membrane packing density. As shown in Table 2, the R1-HP reactor with higher packing density has higher water productivity and 61% lower energy consumption. But it has lower permeate flux (~ 30% lower than R2-LP), thus more membrane areas are required, which results in 44% higher membrane cost. As a result, the total cost (operating cost + capital cost) of R1-HP was 26% higher than that of R2-LP, therefore the biocarriers facilitated GDM reactor with lower membrane packing density is preferred for lower cost of wastewater treatment. In addition, assuming a linear relationship between permeate flux and membrane packing density

within the range of this study, ~360 m^2/m^3 was predicted as the optimal membrane packing density with the lowest total cost (Figure S4).

Clearly, the membrane packing density, closely linked to the recirculation ratio, HRT, and membrane fouling, could impact the water quality, membrane performance, and treatment cost. To reduce the membrane cost per unit volume of treated water (i.e., accounted for 83-95% of total cost in this study for a biocarriers facilitated GDM), the low packing density membrane module was favorable to achieve higher permeate flux. Thus, further research is necessary to optimize membrane packing density towards reducing the membrane cost and reactor footprint without significantly compromising the water productivity and treatment performance.

Table 2. The energy consumption and wastewater treatment cost of R1-HP and R2-LP.

		R1-HP	R2-LP
Permeate water productivity (m^3/d)		0.223	0.081
Permeate flux ($L/m^2/h$)		3.1	4.5
Energy consumption (kWh/m^3)	Feed pump	0.003	0.003
	Recirculation pump	0.010	0.027
	Aeration	0.020	0.056
	Total	0.034	0.087
Capital cost ($Euro/m^3$)	Membranes[a]	0.182	0.127
	Biocarriers (GAC)[b]	0.003	0.007
	Recirculation pump[c,d]	0.0006	0.0016
	Others[c] (feed pump[d], blower, and reactor construction)	0.003	0.008
	Total	0.189	0.144
Operating cost ($Euro/m^3$)	Energy[e]	0.003	0.009
Total cost ($Euro/m^3$)		0.192	0.153

[a] Membrane cost and lifespan was assumed to be 50 $Euro/m^2$ and 10 years, respectively (Judd 2010).
[b] GAC cost and lifespan was estimated as 972 Euro/ton and 5 years, respectively (Nguyen et al. 2014).
[c] (Verrecht et al. 2010)
[d] The capacity of feed pump and recirculation pump was assumed to be the same as 40 L/h for both reactors.

[e] Electricity cost was assumed to be 0.1 Euro/kWh.

3.2. Effect of the presence and absence internal recirculation

To confirm the improved performance of GDM reactors with internal recirculation, a comparison of permeate quality and flux of the GDM reactors in this study (with internal recirculation) and those of the GDM reactors in our previous study (under the same operation condition without internal recirculation) (Lee et al. 2019) was performed and shown in Table 3. It is noted that the membrane packing density of the previous GDM reactor was the same as that of current R2-LP (69 cm^2 per module; 87 m^2/m^3).

Table 3. A comparison of permeate water quality and flux in presence and absence of internal recirculation in the biocarriers facilitated GDM reactors.

		Without internal recirculation (Lee et al. 2019)[a]	With internal recirculation	
			R1-HP	R2-LP[a]
Feed	DOC (mg/L)	24.2±7.5	42.3±6.8	
	TN (mg/L)	36.8±4.0	40.0±4.3	
In the reactor	DOC (mg/L) (Removal)	4.4±0.8 (80.6%)	4.7±0.9 (88.5%)	3.6±0.7 (91.4%)
	Ammonia (mg/L) (Removal)	5.3±1.9 (84.7%)	1.2±0.5 (96.9%)	0.8±0.2 (97.9%)
	TN (mg/L) (Removal)	25.6±3.1 (30.3%)	14.3±2.4 (63.8%)	8.5±0.9 (78.6%)
Permeate	DOC (mg/L) (Removal)	3.0±1.8 (85.0%)	2.3±0.9 (94.5%)	3.0±1.4 (92.8%)
	TN (mg/L) (Removal)	25.1±2.3 (31.5%)	13.8±2.7 (65.1%)	7.9±0.9 (79.8%)
Stabilized flux (LMH)		~2.0	~3.1	~4.5
Cake layer resistance (m^{-1})		4.02×10^{12}	1.72×10^{11}	0.94×10^{11}

[a] In both reactors, the membrane module had the same packing density.

In the presence of internal recirculation, the DOC removal ratios (92.8-94.5%) and TN removal ratio (65.1-79.8%) were obviously greater than those without internal recirculation (85.0% for DOC removal and 31.5% for TN removal). The improved removal efficiencies of DOC and

ammonia in this study were attributed not only by enhanced biodegradation of the GAC biocarriers in the presence of internal recirculation, but also by additional biodegradation contribution of the moving biocarriers (Figure S3). In the previous study (Lee et al., 2019) without additional moving biocarriers and internal recirculation, DO levels in the GDM reactor were comparable to that in this study (with additional moving biocarriers and internal recirculation). Therefore, additional moving biocarriers may not contribute greatly to denitrification (limited by such high DO levels). Indeed, the presence of internal recirculation allowed the nitrate formed in GAC-free zone (high DO and low DOC) being introduced to the GAC layer (low DO and high DOC), leading to an enhanced denitrification. As a result, total nitrogen removal was improved with internal recirculation.

In addition, the presence of internal recirculation in the GDM reactors also benefited to achieve a higher level of stabilized flux. In particular, the internal recirculation led to a greatly decrease of biofilm cake layer resistance (0.94×10^{11} m^{-1} with internal recirculation *vs.* 4.02×10^{12} m^{-1} without internal recirculation). Previous studies have pointed out that the permeability of GDM systems was closely associated with the organic concentration (Peter-Varbanets et al. 2010, Tang et al. 2018). In this study, the organic concentrations in the reactors were comparable, regardless of the presence or absence of internal recirculation (~3.6-4.7 mg DOC/L with internal recirculation *vs.* ~4.4 mg DOC/L without internal recirculation) (Table 3). Thus, the different permeate fluxes in the presence and absence of internal recirculation may not be associated with DOC levels in the biocarriers facilitated GDM systems. It has been well documented that biodegradable dissolved organic carbon (BDOC) and assimilable organic carbon (AOC) played important roles in promoting biofouling although BDOC and AOC accounted for only ~10-30% and <1% of total DOC, respectively (Escobar and Randall 2001, Pramanik et al. 2015). Furthermore, Pramanik et al. (2015) pointed out that the biological

activated carbon process could effectively remove both BDOC and AOC due to enhanced biodegradation. Possibly, although the DOC levels were similar for both conditions, the contents of BDOC and AOC in the GDM reactors with internal recirculation could be lessened because the microorganisms attached on the GAC facilitated biodegradation of BDOC and AOC. As a result, an improved permeate flux with limited biofilm fouling resistance could be achieved in the GDM reactors with internal recirculation. Overall, the presence of internal recirculation significantly improved water quality and membrane performances with a negligible increase of the total wastewater treatment cost (~1-3%, Table 2).

On the other hand, in this study, similar microbial community structures in the GAC particles and on the membrane surfaces were noticed, which was inconsistent with the previous finding in the GDM reactors without internal recirculation and moving biocarriers (i.e., significant differences of both prokaryotic and eukaryotic communities in the GAC particles and on the membrane surfaces) (Lee et al. 2019). Possibly, the internal recirculation could create less dissimilar conditions (such as dissolved oxygen, organic concentrations) for microbial proliferation inside of the reactor, leading to similar microbial composition. In addition, in the presence of internal recirculation, dissolved oxygen was introduced from the aeration zone into the GAC layer. Accordingly, the obligate or facultative anaerobic bacteria present in the GAC layer were relatively lower compared to those without internal recirculation (e.g., only 1.5-2.5% of Clostridia with recirculation *vs.* 20.8% of Clostridia, 6.7% of *Anaeroplasma*, 1.5% of *Lactobacillus*, 1.2% of *Bacterioides* without recirculation).

4. Conclusions

In this study, the effects of internal recirculation and membrane packing density on the reactor performance of the biocarriers facilitated GDM systems were studied. The presence of internal

418 recirculation could effectively improve the permeate water quality and membrane performance.
419 In addition, in the presence of internal recirculation, the low membrane packing density with
420 the longer HRT and higher recirculation ratio could result in higher nitrogen removal ratios,
421 enhanced membrane permeability, and reduced wastewater treatment cost. While, the
422 membrane packing density did not significantly affect DOC removal efficiency and microbial
423 community compositions.

424 **Acknowledgements**

425 The Economic Development Board (EDB) of Singapore is acknowledged for funding the
426 Singapore Membrane Technology Centre (SMTC), Nanyang Technological University. The
427 authors express their gratitude to Prof. Eberhard Morgenroth at Institute of Environmental
428 Engineering of ETH Zürich (Switzerland) for his advice and support.

429

References

Alleman, J. (1985) Elevated nitrite occurrence in biological wastewater treatment systems. Water science and technology 17(2-3), 409-419.

Braak, E., Alliet, M., Schetrite, S. and Albasi, C. (2011) Aeration and hydrodynamics in submerged membrane bioreactors. Journal of Membrane Science 379(1), 1-18.

Broeckmann, A., Busch, J., Wintgens, T. and Marquardt, W. (2006) Modeling of pore blocking and cake layer formation in membrane filtration for wastewater treatment. Desalination 189(1), 97-109.

Caporaso, J.G., Kuczynski, J., Stombaugh, J., Bittinger, K., Bushman, F.D., Costello, E.K., Fierer, N., Peña, A.G., Goodrich, J.K., Gordon, J.I., Huttley, G.A., Kelley, S.T., Knights, D., Koenig, J.E., Ley, R.E., Lozupone, C.A., McDonald, D., Muegge, B.D., Pirrung, M., Reeder, J., Sevinsky, J.R., Turnbaugh, P.J., Walters, W.A., Widmann, J., Yatsunenko, T., Zaneveld, J. and Knight, R. (2010) QIIME allows analysis of high-throughput community sequencing data. Nature Methods 7(5), 335-336.

Characklis, W.G. (1981) Bioengineering report: fouling biofilm development: a process analysis. Biotechnology and Bioengineering 23(9), 1923-1960.

Deng, L., Guo, W., Ngo, H.H., Zhang, X., Wang, X.C., Zhang, Q. and Chen, R. (2016) New functional biocarriers for enhancing the performance of a hybrid moving bed biofilm reactor–membrane bioreactor system. Bioresource technology 208, 87-93.

Derlon, N., Koch, N., Eugster, B., Posch, T., Pernthaler, J., Pronk, W. and Morgenroth, E. (2013) Activity of metazoa governs biofilm structure formation and enhances permeate flux during Gravity-Driven Membrane (GDM) filtration. Water Research 47(6), 2085-2095.

Ding, A., Liang, H., Li, G., Derlon, N., Szivak, I., Morgenroth, E. and Pronk, W. (2016) Impact of aeration shear stress on permeate flux and fouling layer properties in a low pressure membrane bioreactor for the treatment of grey water. Journal of Membrane Science 510, 382-390.

Ding, A., Wang, J., Lin, D., Tang, X., Cheng, X., Li, G., Ren, N. and Liang, H. (2017) In situ coagulation versus pre-coagulation for gravity-driven membrane bioreactor during decentralized sewage treatment: Permeability stabilization, fouling layer formation and biological activity. Water Research 126, 197-207.

Escobar, I.C. and Randall, A.A. (2001) Assimilable organic carbon (AOC) and biodegradable dissolved organic carbon (BDOC):: complementary measurements. Water Research 35(18), 4444-4454.

Huber, S.A., Balz, A., Abert, M. and Pronk, W. (2011) Characterisation of aquatic humic and non-humic matter with size-exclusion chromatography – organic carbon detection – organic nitrogen detection (LC-OCD-OND). Water Research 45(2), 879-885.

Jabornig, S. and Podmirseg, S.M. (2015) A novel fixed fibre biofilm membrane process for on- site greywater reclamation requiring no fouling control. Biotechnology and bioengineering 112(3), 484-493.

Judd, S. (2010) The MBR book: principles and applications of membrane bioreactors for water and wastewater treatment, Elsevier.

Klein, T., Zihlmann, D., Derlon, N., Isaacson, C., Szivak, I., Weissbrodt, D.G. and Pronk, W. (2016) Biological control of biofilms on membranes by metazoans. Water Research 88, 20-29.

Künzle, R., Pronk, W., Morgenroth, E. and Larsen, T.A. (2015) An energy-efficient membrane bioreactor for on-site treatment and recovery of wastewater. Journal of Water, Sanitation and Hygiene for Development 5(3), 448-455.

Lee, S., Sutter, M., Burkhardt, M., Wu, B. and Chong, T.H. (2019) Biocarriers facilitated gravity-driven membrane (GDM) reactor for wastewater reclamation: Effect of intermittent aeration cycle. Science of the Total Environment 694, 133719.

Maere, T., Verrecht, B., Moerenhout, S., Judd, S. and Nopens, I. (2011) BSM-MBR: A benchmark simulation model to compare control and operational strategies for membrane bioreactors. Water Research 45(6), 2181-2190.

Nguyen, A.V., Pham, N.T., Nguyen, T.H., Morel, A. and Tonderski, K. (2007) Improved septic tank with constructed wetland, a promising decentralized wastewater treatment alternative in Vietnam.

Nguyen, T.V., Jeong, S., Pham, T.T.N., Kandasamy, J. and Vigneswaran, S. (2014) Effect of granular activated carbon filter on the subsequent flocculation in seawater treatment. Desalination 354, 9-16.

Peinemann, K.-V. and Nunes, S.P. (2010) Membranes for water treatment, John Wiley & Sons.

501 Peter-Varbanets, M., Hammes, F., Vital, M. and Pronk, W. (2010) Stabilization of flux during dead-
502 end ultra-low pressure ultrafiltration. Water Research 44(12), 3607-3616.
503
504 Pramanik, B.K., Roddick, F.A., Fan, L., Jeong, S. and Vigneswaran, S. (2015) Assessment of biological
505 activated carbon treatment to control membrane fouling in reverse osmosis of secondary effluent for
506 reuse in irrigation. Desalination 364, 90-95.
507
508 Pronk, W., Ding, A., Morgenroth, E., Derlon, N., Desmond, P., Burkhardt, M., Wu, B. and Fane, A.G.
509 (2019) Gravity-driven membrane filtration for water and wastewater treatment: A review. Water
510 research 149, 553-565.
511
512 Rhee, S.-K., Lee, J.J. and Lee, S.-T. (1997) Nitrite accumulation in a sequencing batch reactor during
513 the aerobic phase of biological nitrogen removal. Biotechnology Letters 19(2), 195-198.
514
515 Seidel, A. and Elimelech, M. (2002) Coupling between chemical and physical interactions in natural
516 organic matter (NOM) fouling of nanofiltration membranes: implications for fouling control. Journal
517 of Membrane Science 203(1), 245-255.
518
519 Tang, X., Pronk, W., Ding, A., Cheng, X., Wang, J., Xie, B., Li, G. and Liang, H. (2018) Coupling
520 GAC to ultra-low-pressure filtration to modify the biofouling layer and bio-community: flux
521 enhancement and water quality improvement. Chemical Engineering Journal 333, 289-299.
522
523 Verrecht, B., Maere, T., Nopens, I., Brepols, C. and Judd, S. (2010) The cost of a large-scale hollow
524 fibre MBR. Water Research 44(18), 5274-5283.
525
526 Wang, Y., Fortunato, L., Jeong, S. and Leiknes, T. (2017) Gravity-driven membrane system for
527 secondary wastewater effluent treatment: Filtration performance and fouling characterization.
528 Separation and Purification Technology 184, 26-33.
529
530 Wu, B., Christen, T., Tan, H.S., Hochstrasser, F., Suwarno, S.R., Liu, X., Chong, T.H., Burkhardt, M.,
531 Pronk, W. and Fane, A.G. (2017) Improved performance of gravity-driven membrane filtration for
532 seawater pretreatment: Implications of membrane module configuration. Water Research 114, 59-68.
533
534 Wu, B., Soon, G.Q.Y. and Chong, T.H. (2019) Recycling rainwater by submerged gravity-driven
535 membrane (GDM) reactors: Effect of hydraulic retention time and periodic backwash. Science of the
536 Total Environment 654, 10-18.

537

Graphical Abstract

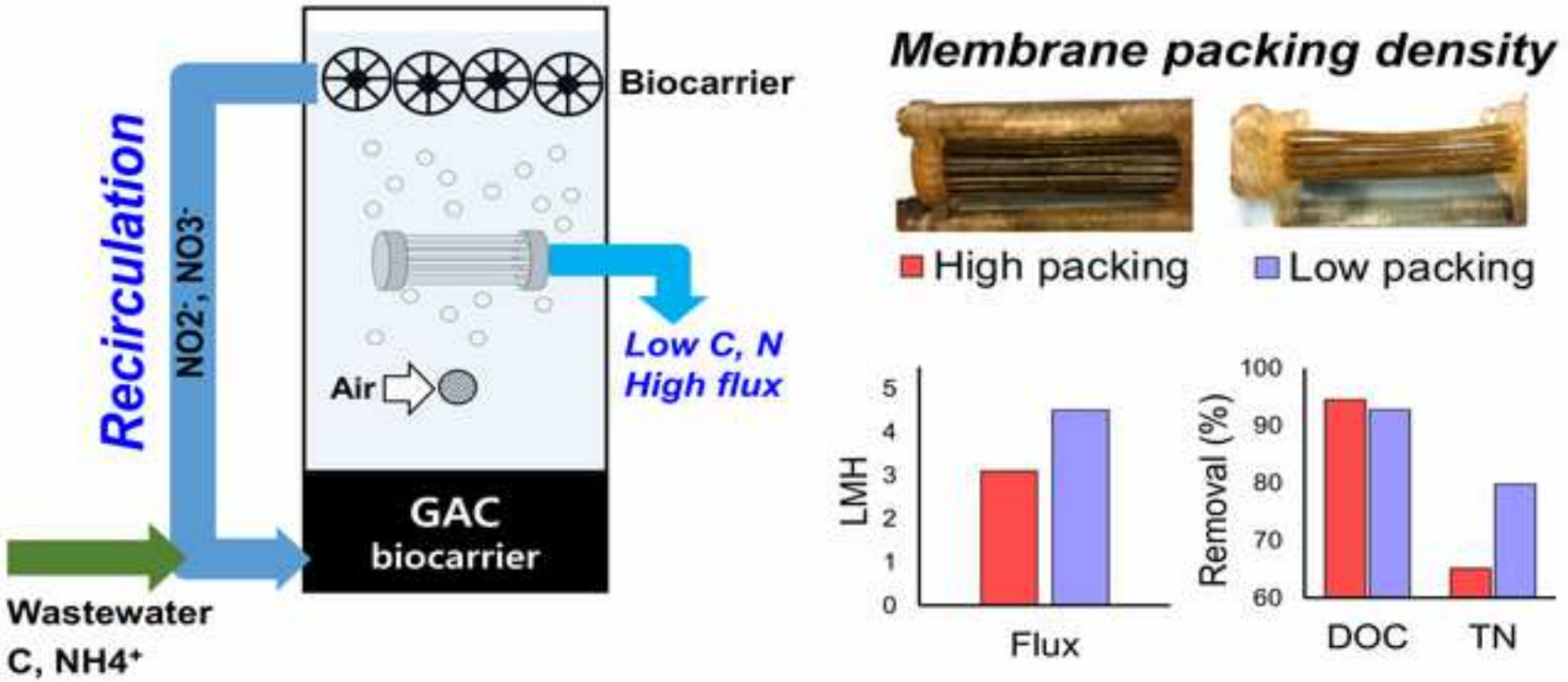

Highlights

1. GDM reactor with internal recirculation had better water quality and higher flux
2. Internal recirculation influenced microbial community in GDM reactor
3. GDM reactor with loose-packed module improved nitrogen removal and permeate flux
4. Membrane packing density had no impact on microbial community in GDM reactor
5. GDM reactor with loose-packed module showed economic benefits

Enhancing Performance of Biocarriers Facilitated Gravity-Driven Membrane (GDM) Reactor for Decentralized Wastewater Treatment: Effect of Internal Recirculation and Membrane Packing Density

Seonki Lee [a,b], Guillaume Olivier Badoux [c,d], Bing Wu [a,e,*], Tzyy Haur Chong [a,b,**]

[a] Singapore Membrane Technology Centre, Nanyang Environment and Water Research Institute, Nanyang Technological University, 1 Cleantech Loop, Clean Tech One 06-08, Singapore 637141

[b] School of Civil and Environmental Engineering, Nanyang Technological University, 50 Nanyang Avenue, Singapore 639798

[c] Eawag, Swiss Federal Institute of Aquatic Science and Technology, 8600, Dübendorf, Switzerland

[d] ETH Zürich, Institute of Environmental Engineering, 8093, Zürich, Switzerland

[e] Faculty of Civil and Environmental Engineering, University of Iceland, Hjardarhagi 2-6, IS-107 Reykjavik, Iceland

*Corresponding author: E-mail: wubing@hi.is

**Corresponding author: E-mail: THChong@ntu.edu.sg

Abstract

This study aims to investigate the effect of internal recirculation and membrane packing density on the performance (water quality, membrane performance, and microbial community) of a biocarriers facilitated gravity-driven membrane (GDM) reactor under intermittent aeration condition. The results revealed that the presence of internal recirculation in the GDM reactors could effectively improve water quality (especially increasing nitrogen removal) and membrane performance (especially reducing cake layer resistance) compared to those without internal recirculation. In addition, compared to a high packing density membrane module (1150 m^2/m^3), a lower packing density membrane module (290 m^2/m^3) benefited to improve 15% of nitrogen removal and 44% of permeate flux due to the effective aeration scouring effect and less-limited eukaryotic activity, as well as reduce 20% of total treatment cost. In addition, the presence and absence of internal recirculation could lead to dissimilar microbial community compositions of the biofilms in the GAC layers and on the membrane surfaces. However, the membrane packing density could play an insignificant effect on the microbial community compositions of the biofilms in the GDM reactors with internal recirculation.

Keywords: Decentralized wastewater treatment; Gravity-driven membrane; Recirculation; Membrane packing density; Nitrogen removal

1. Introduction

Decentralized wastewater treatment systems have been considered as an adoptable option in rural areas and developing countries due to their inexpensive installation, easy operation, and low operating and maintaining cost. Traditional decentralized systems, such as constructed wetland and septic tank, have been well applied in treating wastewater, however, nowadays they are facing challenges due to their limit in meeting the increasingly strict discharge standards (Nguyen et al. 2007).

Recently, gravity-driven membrane (GDM) reactors have been developed as an alternative decentralized system in treating greywater/municipal wastewater (Ding et al. 2016, Ding et al. 2017, Jabornig and Podmirseg 2015, Künzle et al. 2015, Lee et al. 2019, Wang et al. 2017). The GDM reactor is a membrane-based process driven by natural hydrostatic gravity force, therefore, it can produce superior permeate water without requiring permeate suction pump and membrane chemical cleaning protocols. This guarantees that the GDM can be operated with significantly lower energy consumption and capital cost than conventional membrane bioreactors. It has been well illustrated that the stabilized permeate flux achieved in the GDM reactor was attributed to the heterogeneous biofilm layer formed on the membrane surface, in which organic degradation, prokaryotes proliferation, and eukaryotes movement/predation occurred and their contributions to the biofilm formation displayed a relatively steady pattern (Peter-Varbanets et al. 2010, Tang et al. 2018).

However, GDM reactors had relatively lower permeate fluxes (<10 $L/m^2/h$) in treating wastewater due to lower driving force and limited biodegradation of organics. To further improve permeate flux, integrating GDM reactors with aeration, coagulation, and biocarriers have been well documented (Ding et al. 2017, Jabornig and Podmirseg 2015, Künzle et al. 2015, Lee et al. 2019). In a previous study (Lee et al. 2019), we developed a hybrid upflow

packed-bed granular activated carbon (GAC) facilitated GDM reactor and operated it at an intermittent aeration mode (aeration diffuser was located above the GAC bed). The results showed that this combination could effectively improve membrane performance as well as the organic (87.8-90.5%) and nitrogen removal (29.3-37.1%) compared to the GDM reactor without intermittent aeration. It was also found that intermittent aeration could negatively influence the nitrogen removal efficiency because (1) a high level (~3.5 mg/L) of residual dissolved oxygen (DO) in the membrane zone during non-aeration period resulted in poor denitrification of the biofilm attached on the membrane; and (2) the anoxic biofilm on the GAC carriers had limited contribution to denitrification due to less available nitrite/nitrate. Thus, to maximize nutrient removal in the GAC+GDM reactors, installation of internal recirculation in the reactor could be considered, aiming to deliver nitrite/nitrate-contained effluent in the intermittent aeration zone to the anoxic GAC zone and enhance denitrification of the biofilm on the GAC carriers. Meanwhile, it has been reported that sponge modified plastic carriers facilitated immobilizing more microorganisms due to their high porosity nature and improving organic and nutrient removals in moving bed biofilm reactor systems (Deng et al. 2016).

In addition, compared to MBRs, the GAC+GDM reactors had lower permeate fluxes. Therefore, a GAC+GDM reactor requires more membrane area with a higher membrane packing density than a conventional submerged MBR under the same water productivity and footprint scenarios. It has been reported that the high packing density of membrane module in MBRs suffered more serious fouling due to ineffective air scouring (Braak et al. 2011). The non-aeration GDM systems with high packing density hollow fibre membrane modules also had lower permeate fluxes in pre-treating seawater, possibly because of limited predation and movement behaviors of eukaryotes between the insufficient space of hollow fibres (Wu et al. 2017). Furthermore, the membrane packing density (i.e., membrane area) determined hydraulic retention time (HRT)

of the GDM reactors, which was also associated with water quality (Wu et al. 2019). Thus, it is necessarily important to optimize the membrane module density in the GAC+GDM reactors in order to maximize wastewater treatment capability with reduced footprint.

In this study, internal recirculation and moving biocarriers were introduced to the biocarriers facilitated GDM system in treating municipal wastewater to enhance the reactor performance (nutrient removal and permeate flux). In addition, the effect of membrane packing density on water quality, membrane performance, microbial community, and cost were examined.

2. Materials and methods

2.1. Setup and operating conditions of biocarriers facilitated GDM reactors

Two laboratory-scale biocarriers facilitated GDM reactors (working volume of 8.6 L) with internal recirculation were operated in parallel. As shown in Figure 1, the GAC biocarriers (1.25 kg; Filtrasorb 300, US) were placed on the bottom of the reactor, and the Kaldnes K3 plastic biocarriers (120 pcs; China) that were modified by inserting a sponge cube (10 mm × 10 mm, Aquaporous Gel, Japan) into a plastic biocarrier's void space were floated on the top of the reactor (Deng et al. 2016). Two identical hollow fiber membrane modules (PVDF; 150 kDa) were installed at ~30 cm below the water level (i.e., a hydrostatic pressure of ~30 mbar). An air diffuser was located between the GAC layer and the membrane modules. Intermittent aeration (30 min aeration at 0.5 L/min followed by 60 min non-aeration) was delivered into the GDM reactor by using a timer-controlled aeration pump (Lee et al. 2019). The feed wastewater was introduced from the feed tank to the bottom of the reactor by a peristaltic pump and its flow rate was manually adjusted according to the permeate flow rate in order to minimize the overflow. The mixed liquor at the top of the reactor was recirculated back to the bottom of the reactor using a peristaltic pump with a constant flow rate (0.52 L/h).

In one reactor (hereinafter R1-HP), two membrane modules with the high membrane packing density (1150 m^2/m^3; membrane area of 268 cm^2 per module) were installed, while in the other reactor (hereinafter R2-LP), two membrane modules with the low packing density (290 m^2/m^3; membrane area of 69 cm^2 per module) were employed (Table 1). The feed wastewater was collected from the primary clarifier in the Ulu Pandan Wastewater Reclamation Plant in Singapore. There was no sludge discharge and membrane cleaning during the whole period of operation. The room temperature was kept at 20°C.

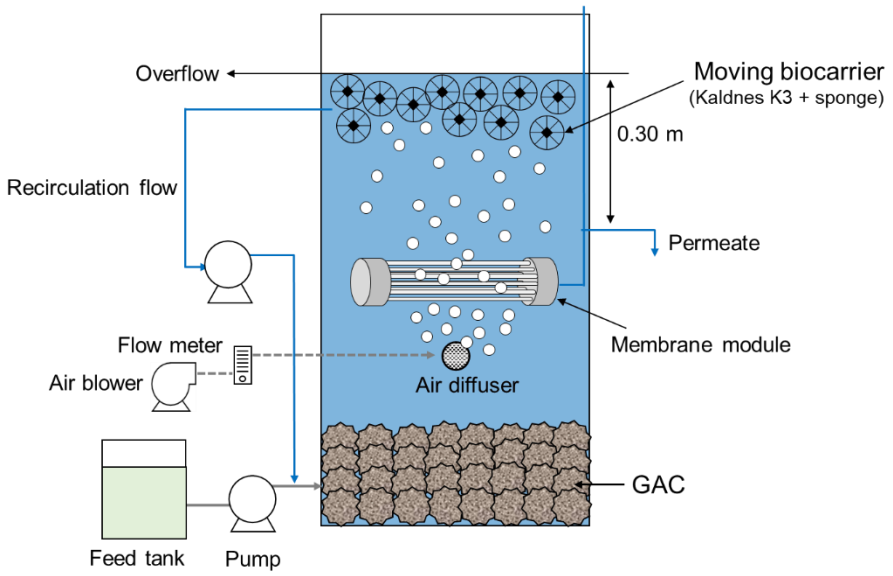

Figure 1. A schematic diagram of the biocarriers facilitated GDM reactor.

Table 1. Operating conditions of the biocarriers facilitated GDM reactors.

	R1-HP	R2-LP
pH	7.3±0.4	7.2±0.2
DO (mg/L)	3.4±0.7	3.8±0.9
Effective total membrane area (cm^2)	536	138
Membrane packing density (m^2/m^3)	1150	290
Averaged HRT[a] (h)	~59	~154
Averaged recirculation ratio[b]	~3.5	~9.2

[a] HRT was determined daily and averaged HRT was calculated by averaging the daily HRT.
[b] The recirculation ratio was defined as the ratio of recirculation flow rate (0.52 L/h) to the feed flow rate. Averaged recirculation ratio was calculated by averaging the daily recirculation ratio.

2.2. Water quality analysis

The feed, reactor, and permeate samples were periodically collected and then filtered with 0.45 μm syringe membranes (Millipore, USA) and filtrate was kept at 4℃ before analysis. The dissolved organic carbon (DOC) and total nitrogen (TN) were determined using a TOC/TN analyzer (TOC-VCSH/TNM-1, Shimadzu, Japan). Soluble organic fractions in the water samples were determined by an LC-OCD analyzer (LC-OCD Model 8, DOC-LABOR, Germany), a size-exclusion chromatography coupled with organic carbon detector and organic nitrogen detector. According to the molecular weight, the organic fractions were classified into five groups, i.e., biopolymers (MW > 20 kDa), humic substances (MW ~1000 Da), building blocks (MW ~300-500 Da), low molecular weight (LMW) acids and neutrals (MW < 350 Da). The details in operation and analysis procedures were referred from the literature (Huber et al. 2011).

Ammonia (NH_4-N), nitrite (NO_2-N), and nitrate (NO_3-N) were measured using the spectrometric method with Ammonia TNT 830, 831, 832 kit (Hach, USA), Nitrite LCK 341 kit (Hach Lange GmbH, Germany), and Nitrate TNT 835 kit (Hach, USA), respectively. The pH and dissolved oxygen (DO) were periodically monitored using a portable pH meter (Mettler Toledo, Switzerland) and a portable DO meter (Mettler Toledo, Switzerland), respectively.

To illustrate the statistical significance, a two-sample t-test was conducted by comparing the sampling data groups under two different conditions. The p-values for the two-sample t-test were calculated at a significance level of 0.05.

2.3. Fouling resistance

To characterize the membrane fouling, the fouling resistance was evaluated based on the resistance-in-series model (Broeckmann et al. 2006). At the end of experiment (the total resistance R_t was calculated based on the final permeate flux), the membrane module was

147 removed from the reactor, and cake layer was physically detached by rinsing with Milli-Q
148 water for 10 min and followed by sonication for 15 min. Then, the permeate flux of the
149 physically-cleaned membrane was measured at the hydrostatic pressure of 30 mbar and the
150 resistance was calculated as $(R_m + R_{ir})$. The biofilm cake resistance (R_c) was obtained by
151 subtracting the resistance after physical cleaning $(R_m + R_{ir})$ from the total resistance (R_t). In
152 addition, the irreversible fouling resistance (R_{ir}) was achieved by subtracting the intrinsic
153 membrane resistance (R_m) from the resistance after physical cleaning $(R_m + R_{ir})$.

154 **2.4. Microbial community**

155 At the end of experiment, biofilms were collected from the membrane module, GAC biocarriers,
156 moving biocarriers (i.e. Kaldnes K3 with sponge), and then kept at -20℃ before DNA
157 extraction. Genomic DNA was extracted from biofilms using PowerSoil® DNA isolation kit
158 (MO bio, USA). The prokaryotic and eukaryotic microbial communities in biofilms were
159 analyzed using the 16S and 18S rRNA sequencing, respectively, on the Illumina MiSeq
160 platform. Primers 357wF (CCTACGGGGNGGCWGCAG) and 785R
161 (GACTACHVGGGTATCTAATCC) for prokaryotes, TAReukF
162 (CCAGCASCYGCGGTAATTCC) and TAReukR (ACTTTCGTTCTTGATYRA) eukaryotes
163 were chosen. The sequencing results were analyzed by the standard de novo operational
164 taxonomic unit (OTU)-based approach using QIIME software (Caporaso et al. 2010).

165 **3. Results and Discussion**

166 **3.1. Effect of membrane packing density**

167 3.1.1. Organic removal

168 Both GDM reactors were operated in parallel for 45 days. As the feed water flow was daily

regulated based on the permeate flow (i.e., minimizing overflow), within 45-day operation, R1-HP and R2-LP achieved dissimilar HRTs and internal recirculation ratios due to different membrane packing densities (i.e., membrane areas) (Table 1). Increasing membrane packing density led to a decreased HRT (~59 h for R1-HP *vs.* ~154 h for R2-LP) and internal recirculation ratio (~3.5 for R1-HP *vs.* ~9.2 for R2-LP). However, both HRT and internal recirculation ratio parameters did not impact pH and DO levels in the reactors.

Figure 2 shows the DOC concentrations in the feed, reactor and permeate. The DOC in the feed ranged ~24-53 mg/L (averaged at 39.0 mg/L) throughout the whole period of experiment. During the early stage (from Day 0-20), the DOC level in the R1-HP (~6.3-10.7 mg DOC/L) was higher than that of R2-LP (~3.3-6.8 mg DOC/L). This indicated that the shorter HRT and lower recirculation ratio of R1-HP could result in slightly lower organic removal efficiency during the early stage (~79.0% for R1-HP *vs.* ~88.1% for R2-LP; $p<0.05$), possibly associating with the suppressed biodegradation capacity under higher organic loading (shorter HRT). However, the DOC levels in R1-HP decreased with extending operation time (~3.4-6.3 mg/L), showing gradually enhanced biodegradation efficiency. In addition, LC-OCD analysis revealed that with extending operation time, the removal efficiency of biopolymers in R1-HP increased from ~16% (Day 0-20) to ~58% (Day 21-45), while those of humic substances, building blocks, LMW neutrals, and LMW acids were relatively constant (Figure 3). This illustrated that the improved biodegradation of biopolymers contributed to the increasing organic removal efficiency. After both reactors reached the stable stage, they achieved the comparable biodegradable DOC removal ratio (~88.5% for R1-HP *vs.* ~91.4% for R2-LP; $p>0.05$).

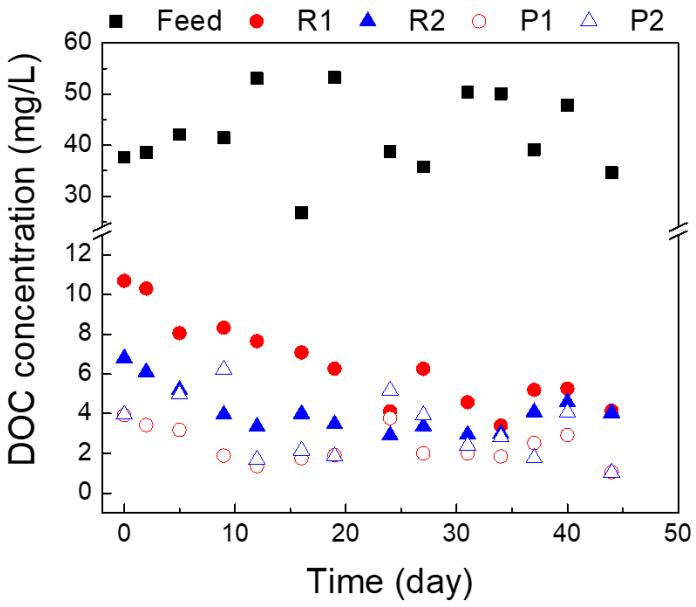

Figure 2. DOC concentrations in the feed, reactor, permeate of R1-HP and R2-LP. R and P represent reactor and permeate, respectively.

In addition, in both GDM reactors, the DOC levels in the permeates (~2.3-3.0 mg DOC/L) were only slightly lower than those in the reactors (~3.6-4.7 mg DOC/L, Figure 2), which suggested that membrane separation contributed only ~1-6% of the overall DOC removal. As shown in the Figure 3, the biopolymers in the permeate were much less than those in the reactors, showing that part of biopolymers could be effectively retained by the membrane. On the other hand, the concentrations of small-sized organics, such as humic substances, building blocks, and LMW acids, were relatively comparable in the reactor and in the permeate. In addition, LMW neutrals concentrations in the permeates were higher than those in the reactors. Possibly, the greater-sized organic matters on the membrane were hydrolyzed or biodegraded (by the biofilm) to small-sized soluble organic molecules, which could pass through the membrane and presented in the permeate. Similar findings were also observed in the previous GDM studies (Lee et al. 2019, Pronk et al. 2019). Nevertheless, both reactors achieved comparable organic levels in the permeate (2.3±0.9 mg/L for R1-HP and 3.0±1.4 mg/L for R2-LP; $p>0.05$).

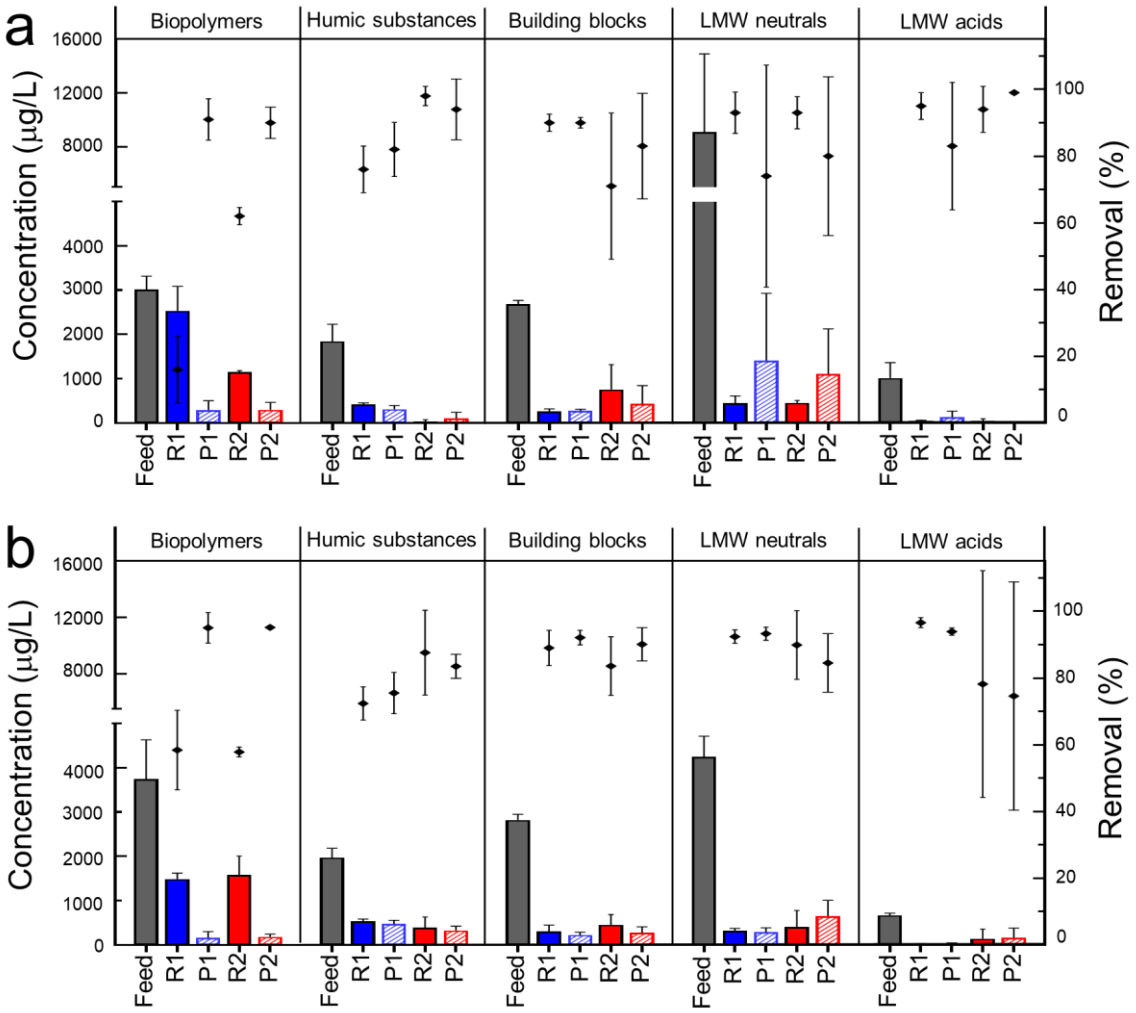

Figure 3. Soluble organic fractions in the feed, reactor, and permeate of R1-HP and R2-LP. (a) during initial stage (Day 0-20, n=2), and (b) during stable stage (Day 21-45, n=3). Columns indicate the concentrations while dots indicate the removal efficiency calculated based on the data in the feed. R and P represent reactor and permeate, respectively.

3.1.2. Nitrogen removal

Figure 4 shows the nitrogen concentrations in feed, reactor, and permeate in both reactors. At the initial period (Day 0-9), total nitrogen (TN) was not effectively removed in both reactors due to poor nitrification (Figures 4a and b). However, during Day 9-12, the performance of nitrification process was remarkably improved, in which the ammonia was mainly converted to nitrite (up to ~7 mg NO_2-N/L, Figure 4c) instead of nitrate (Figure 4d). Afterwards, only very limited ammonia were detected in both reactors (~1.2±0.5 mg NH_4-N/L for R1-HP and

~0.8±0.2 mg NH_4-N/L for R2-LP), showing complete nitrification in both reactors. Meanwhile, the concentration of nitrite in the reactors decreased gradually, which was converted to nitrate. The temporary nitrite accumulation phenomenon during the initial period can be speculated that the activity of nitrite-oxidizing bacteria (NOB) might be lower than that of ammonia-oxidizing bacteria (AOB). It has been well documented that compared to AOB, NOB was often more susceptible to environmental stress such as an acute concentration or loading of free ammonia (Alleman 1985, Rhee et al. 1997). With extending operation time, the NOB activity was enhanced attributed by the decreased ammonia concentration.

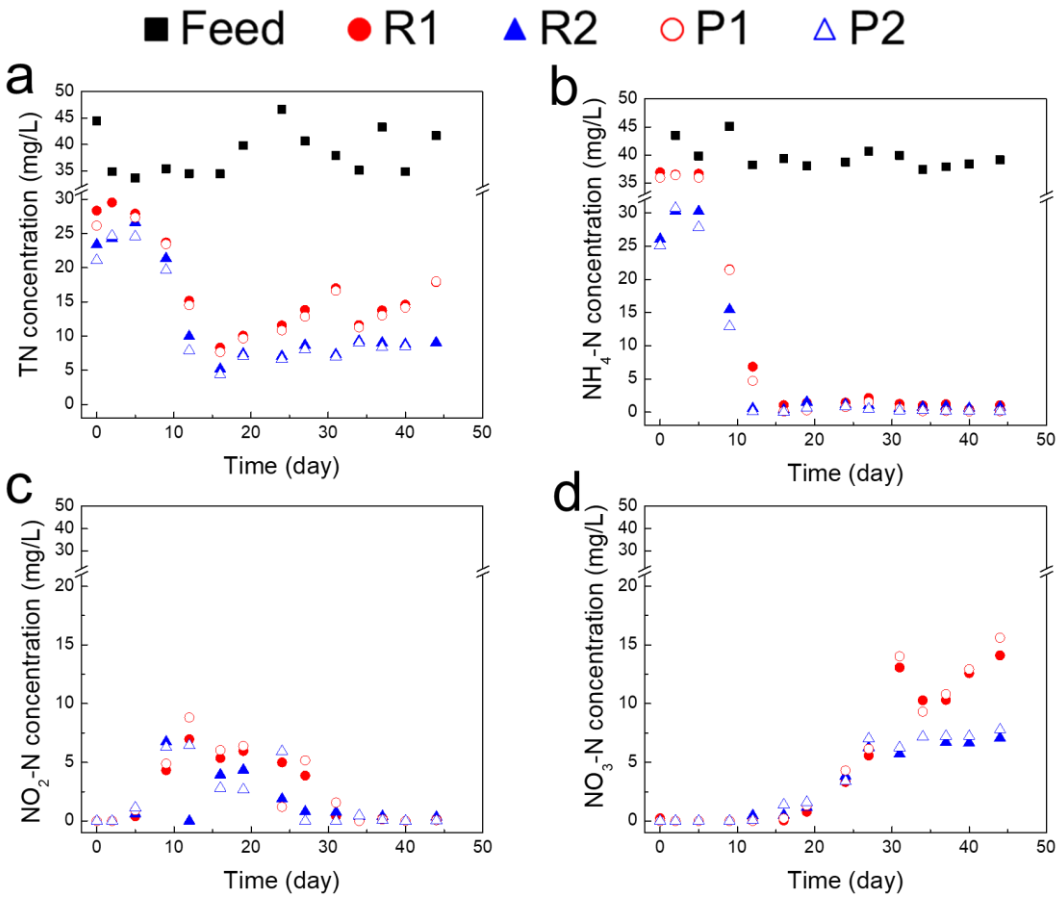

Figure 4. Nitrogen concentrations in the feed, reactor, permeate of R1-HP and R2-LP. (a) TN, (b) Ammonia, (c) Nitrite, (d) Nitrate. R and P represent reactor and permeate, respectively.

Obviously, after Day 20, both reactors had dissimilar concentrations of nitrate and total nitrogen. The lower concentrations of nitrate and total nitrogen were found in R2-LP (~6.2 mg NO_3-N/L and ~8.5 mg TN/L) than those in R1-HP (~9.9 mg NO_3-N/L and ~14.3 mg TN/L). Accordingly, the denitrification ratio of R2-LP (~81.9%) was greater than that of R1-HP (~69.0%), which was associated with the longer HRTs and higher recirculation ratio in R2-LP than R1-HP. As a result, R2-LP achieved the higher biological TN removal efficiency (~78.6%) compared to R1-HP (~63.8%).

In addition, in both reactors, the ammonia and nitrogen concentrations in the permeate were slightly lower than those in the reactor (p<0.05; paired t-test). However, it contributed only about 1-2% of overall ammonia and nitrogen removal performances of the system. It was probably associated with the limited biomass attached on the membrane because of its periodical removal by intermittent aeration.

3.1.3. Membrane performance

Figure 5a shows the permeate fluxes of R1-HP and R2-LP throughout the operation period. The fluxes of both reactors dropped rapidly for the initial 3 days and then followed a slowly-decreased pattern before reaching relatively constant levels. During Day 30-45, the averaged flux of R2-LP was ~4.5 LMH, which was approximately 44% higher than that of R1-HP (~3.1 LMH). This implies that increasing membrane packing density could lead to a decreased permeate flux under intermittent aeration condition. This was consistent with our previous observation for the GDM reactors (hollow fibre modules) in pre-treating seawater under non-aeration condition (Wu et al. 2017). In addition, the water permeability in this study (~103-150 LMH/bar) were slightly higher than those in the reported GDM systems in treating municipal wastewater (~44-118 LMH/bar, Table S1) (Ding et al. 2017, Lee et al. 2019, Peter-Varbanets et al. 2010, Wang et al. 2017).

To explore the membrane fouling mechanism, the membrane resistance, irreversible fouling resistance, and biofilm cake layer resistance were evaluated. As shown in Figure 5b, both reactors had comparable irreversible fouling resistances (1.55×10^{11} m^{-1} for R1-HP and 1.34×10^{11} m^{-1} for R2-LP), while the biofilm cake layer resistance of R2-LP (0.94×10^{11} m^{-1}) was 46% lower than that of R1-HP (1.72×10^{11} m^{-1}). Thus, the lesser biofilm layer resistance of R2-LP resulted in the higher permeate flux. It was probably attributed to three facts: (1) the lower membrane packing density of R2-LP, i.e., having a larger spacing between membrane fibers (Figure S1), which could be more effective in biofilm detachment by the shear stress generated from aeration and thus less effective membrane filtration area was lost (Braak et al. 2011); (2) the lower membrane packing density could also provide sufficient space for eukaryotic predation and movement activities, benefiting to form more heterogeneous cake layer (the confocal laser scanning microscopy images shown in Figure S2) (Derlon et al. 2013, Klein et al. 2016, Wu et al. 2017); (3) the lower DOC levels in R2-LP during the early period (Figure 2) may result in less formation of the organic condition layer, and thereby less biofouling potential in the following stage (Characklis 1981, Seidel and Elimelech 2002).

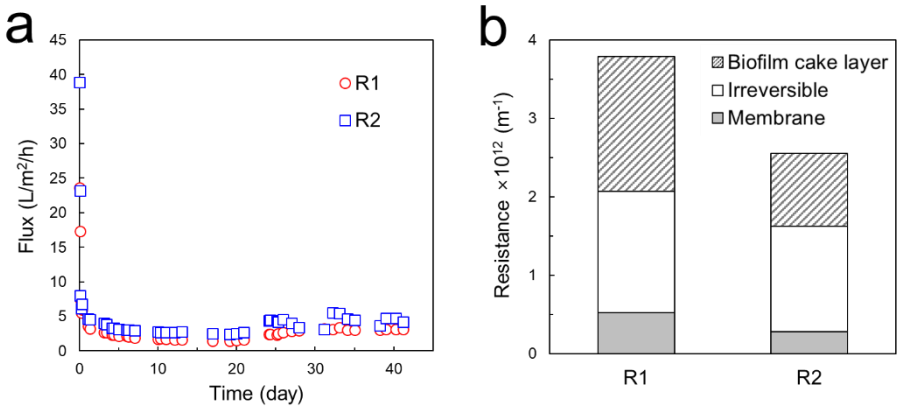

Figure 5. Membrane performances of R1-HP and R2-LP. (a) Permeate flux. (b) Resistance distribution.

3.1.4. Microbial community composition

Figure 6 shows the compositions of prokaryotic and eukaryotic communities in the biofilms derived from GAC particles, moving biocarriers (Kaldnes K3 with sponge), and filtration membranes. In both reactors, Planctomycetes (22.0-47.1%), Proteobacteria (14.2-42.3%), and Verrucomicrobia (12.3-27.3%) were found as major dominant prokaryotic phyla in all biofilms (Figure 6a). In addition, Bacteroidetes and NKB 19, minor dominant phyla, accounted for 1.8-8.4% and 1.4-8.9% respectively, were also detected in all biofilms. These results indicated that the compositions of prokaryotic communities in the biofilms on the GAC, moving biocarriers, and membrane were similar, regardless of membrane packing density.

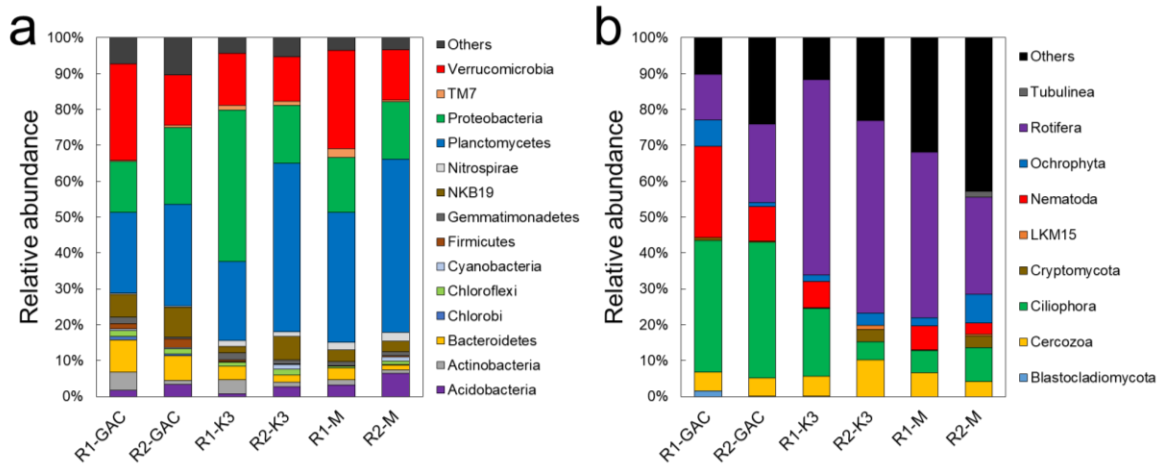

Figure 6. Compositions of prokaryotic (a) and eukaryotic (b) communities in R1-HP and R2-LP. K3 and M represent moving biocarrier (Kaldnes K3 with sponge) and membrane sample, respectively.

As shown in Figure 6b, Rotifera, Ciliophora, Nematoda, and Cercozoa were detected as major eukaryotes in most samples, indicating that the operation conditions (HRT and internal recirculation ratio attributed by membrane packing density) did not influence the predominant compositions of eukaryotic community. However, the abundances of major eukaryotes in the GAC samples were slightly different from those in the moving biocarriers and on the membrane surfaces. In detail, the relative abundances of Ciliophora and Nematoda were much higher in the GAC particles (36.6-37.8% and 9.7-25.4% respectively) than in the moving

biocarriers (5.1-18.8% and ~0-7.4% respectively) and on the membrane surfaces (6.3-9.6% and 3.1-6.7% respectively). In contrast, Rotifera was predominant in the biofilms formed in the moving biocarriers (53.6-54.5%) and on the membrane surfaces (27.1-46.2%), while it was relatively less in the GAC particles (12.7-21.9%). These differences may be derived from the facts that (1) Ciliophora and Nematoda having larger sizes could be trapped within the well-packed GAC layers during recirculation, promoting their accumulations in the GAC particles; and (2) Rotifer may prefer to grow at a relatively higher DO level in the intermittent aeration zone. Nevertheless, the differences in HRTs and internal recirculation ratios caused by different membrane packing densities did not significantly affect the compositions of both prokaryotic community and eukaryotic community.

3.1.5. Energy consumption and water production cost estimation

In this study, the low membrane packing density in the GDM reactor benefited to achieve better membrane performance and improved permeate quality, however it also led to lower water productivity (i.e., wastewater treatment capacity) compared to the high membrane packing density scenario under the same reactor footprint (Table 2). To make a fair comparison, the energy consumption and capital cost of the GDM reactors under different membrane packing density conditions were evaluated and presented in Table 2.

In the energy consumption category, only pump energy and aeration energy were assessed using Eq. (1) and Eq. (2) respectively because the GDM reactors operated without sludge discharge and chemical cleaning in this study.

$$E_{pump} = \frac{\rho g h}{\eta} \frac{Q_{pump}}{Q_p} \qquad (1)$$

$$E_{air} = \frac{\varepsilon Q_{air}}{Q_p} \qquad (2)$$

Where ρ is the density of wastewater (assuming 1000 kg/m^3); g is the gravitational acceleration (9.81 m/s^2); h is the height of water level (0.65 m, i.e., the height between feed pump inlet and water level); η is the pump efficiency (assuming 0.6); ε is the electricity consumption per unit volume of air (assuming 0.019 kWh/m^3 of air) (Maere et al. 2011); Q_{pump} is the flow rate of feed pump or recirculation pump (m^3/s); Q_{air} is the average air flow rate (m^3/s); Q_p is the stabilized permeate flow rate (m^3/s).

The capital cost accounted for reactor construction, pumps, blowers, biocarriers and membranes. The hollow fibre membrane module footprint (1.6-6.2 m^2 membrane area/ m^3 reactor volume) applied in this study were extremely lower than conventional MBRs (<450 m^2/m^3) (Peinemann and Nunes 2010). Therefore, for better estimation of energy consumption and capital cost, it was assumed that 30% of the reactor volume was packed with each membrane module (i.e., 345 m^2 membrane area/m^3 reactor volume in R1-HP and 87 m^2/m^3 in R2-LP). In addition, the average recirculation ratio (3.5 for R1-HP and 9.2 for R2-LP) was used in the estimation of recirculation energy and cost

It is important to recall that in this study, energy input (recirculation and aeration) and footprint (reactor, biocarriers, and other equipment) were identical in both reactors, and the only difference was membrane packing density. As shown in Table 2, the R1-HP reactor with higher packing density has higher water productivity and 61% lower energy consumption. But it has lower permeate flux (~ 30% lower than R2-LP), thus more membrane areas are required, which results in 44% higher membrane cost. As a result, the total cost (operating cost + capital cost) of R1-HP was 26% higher than that of R2-LP, therefore the biocarriers facilitated GDM reactor with lower membrane packing density is preferred for lower cost of wastewater treatment. In addition, assuming a linear relationship between permeate flux and membrane packing density

within the range of this study, ~360 m^2/m^3 was predicted as the optimal membrane packing density with the lowest total cost (Figure S4).

Clearly, the membrane packing density, closely linked to the recirculation ratio, HRT, and membrane fouling, could impact the water quality, membrane performance, and treatment cost. To reduce the membrane cost per unit volume of treated water (i.e., accounted for 83-95% of total cost in this study for a biocarriers facilitated GDM), the low packing density membrane module was favorable to achieve higher permeate flux. Thus, further research is necessary to optimize membrane packing density towards reducing the membrane cost and reactor footprint without significantly compromising the water productivity and treatment performance.

Table 2. The energy consumption and wastewater treatment cost of R1-HP and R2-LP.

		R1-HP	R2-LP
Permeate water productivity (m^3/d)		0.223	0.081
Permeate flux ($L/m^2/h$)		3.1	4.5
Energy consumption (kWh/m^3)	Feed pump	0.003	0.003
	Recirculation pump	0.010	0.027
	Aeration	0.020	0.056
	Total	0.034	0.087
Capital cost (Euro/m^3)	Membranes[a]	0.182	0.127
	Biocarriers (GAC)[b]	0.003	0.007
	Recirculation pump[c,d]	0.0006	0.0016
	Others[c] (feed pump[d], blower, and reactor construction)	0.003	0.008
	Total	0.189	0.144
Operating cost (Euro/m^3)	Energy[e]	0.003	0.009
Total cost (Euro/m^3)		0.192	0.153

[a] Membrane cost and lifespan was assumed to be 50 Euro/m^2 and 10 years, respectively (Judd 2010).

[b] GAC cost and lifespan was estimated as 972 Euro/ton and 5 years, respectively (Nguyen et al. 2014).

[c] (Verrecht et al. 2010)

[d] The capacity of feed pump and recirculation pump was assumed to be the same as 40 L/h for both reactors.

[e] Electricity cost was assumed to be 0.1 Euro/kWh.

3.2. Effect of the presence and absence internal recirculation

To confirm the improved performance of GDM reactors with internal recirculation, a comparison of permeate quality and flux of the GDM reactors in this study (with internal recirculation) and those of the GDM reactors in our previous study (under the same operation condition without internal recirculation) (Lee et al. 2019) was performed and shown in Table 3. It is noted that the membrane packing density of the previous GDM reactor was the same as that of current R2-LP (69 cm^2 per module; 87 m^2/m^3).

Table 3. A comparison of permeate water quality and flux in presence and absence of internal recirculation in the biocarriers facilitated GDM reactors.

		Without internal recirculation (Lee et al. 2019)[a]	With internal recirculation	
			R1-HP	R2-LP[a]
Feed	DOC (mg/L)	24.2±7.5	42.3±6.8	
	TN (mg/L)	36.8±4.0	40.0±4.3	
In the reactor	DOC (mg/L)	4.4±0.8	4.7±0.9	3.6±0.7
	(Removal)	(80.6%)	(88.5%)	(91.4%)
	Ammonia (mg/L)	5.3±1.9	1.2±0.5	0.8±0.2
	(Removal)	(84.7%)	(96.9%)	(97.9%)
	TN (mg/L)	25.6±3.1	14.3±2.4	8.5±0.9
	(Removal)	(30.3%)	(63.8%)	(78.6%)
Permeate	DOC (mg/L)	3.0±1.8	2.3±0.9	3.0±1.4
	(Removal)	(85.0%)	(94.5%)	(92.8%)
	TN (mg/L)	25.1±2.3	13.8±2.7	7.9±0.9
	(Removal)	(31.5%)	(65.1%)	(79.8%)
Stabilized flux (LMH)		~2.0	~3.1	~4.5
Cake layer resistance (m^{-1})		4.02×10^{12}	1.72×10^{11}	0.94×10^{11}

[a] In both reactors, the membrane module had the same packing density.

In the presence of internal recirculation, the DOC removal ratios (92.8-94.5%) and TN removal ratio (65.1-79.8%) were obviously greater than those without internal recirculation (85.0% for DOC removal and 31.5% for TN removal). The improved removal efficiencies of DOC and

ammonia in this study were attributed not only by enhanced biodegradation of the GAC biocarriers in the presence of internal recirculation, but also by additional biodegradation contribution of the moving biocarriers (Figure S3). In the previous study (Lee et al., 2019) without additional moving biocarriers and internal recirculation, DO levels in the GDM reactor were comparable to that in this study (with additional moving biocarriers and internal recirculation). Therefore, additional moving biocarriers may not contribute greatly to denitrification (limited by such high DO levels). Indeed, the presence of internal recirculation allowed the nitrate formed in GAC-free zone (high DO and low DOC) being introduced to the GAC layer (low DO and high DOC), leading to an enhanced denitrification. As a result, total nitrogen removal was improved with internal recirculation.

In addition, the presence of internal recirculation in the GDM reactors also benefited to achieve a higher level of stabilized flux. In particular, the internal recirculation led to a greatly decrease of biofilm cake layer resistance (0.94×10^{11} m^{-1} with internal recirculation *vs.* 4.02×10^{12} m^{-1} without internal recirculation). Previous studies have pointed out that the permeability of GDM systems was closely associated with the organic concentration (Peter-Varbanets et al. 2010, Tang et al. 2018). In this study, the organic concentrations in the reactors were comparable, regardless of the presence or absence of internal recirculation (~3.6-4.7 mg DOC/L with internal recirculation *vs.* ~4.4 mg DOC/L without internal recirculation) (Table 3). Thus, the different permeate fluxes in the presence and absence of internal recirculation may not be associated with DOC levels in the biocarriers facilitated GDM systems. It has been well documented that biodegradable dissolved organic carbon (BDOC) and assimilable organic carbon (AOC) played important roles in promoting biofouling although BDOC and AOC accounted for only ~10-30% and <1% of total DOC, respectively (Escobar and Randall 2001, Pramanik et al. 2015). Furthermore, Pramanik et al. (2015) pointed out that the biological

activated carbon process could effectively remove both BDOC and AOC due to enhanced biodegradation. Possibly, although the DOC levels were similar for both conditions, the contents of BDOC and AOC in the GDM reactors with internal recirculation could be lessened because the microorganisms attached on the GAC facilitated biodegradation of BDOC and AOC. As a result, an improved permeate flux with limited biofilm fouling resistance could be achieved in the GDM reactors with internal recirculation. Overall, the presence of internal recirculation significantly improved water quality and membrane performances with a negligible increase of the total wastewater treatment cost (~1-3%, Table 2).

On the other hand, in this study, similar microbial community structures in the GAC particles and on the membrane surfaces were noticed, which was inconsistent with the previous finding in the GDM reactors without internal recirculation and moving biocarriers (i.e., significant differences of both prokaryotic and eukaryotic communities in the GAC particles and on the membrane surfaces) (Lee et al. 2019). Possibly, the internal recirculation could create less dissimilar conditions (such as dissolved oxygen, organic concentrations) for microbial proliferation inside of the reactor, leading to similar microbial composition. In addition, in the presence of internal recirculation, dissolved oxygen was introduced from the aeration zone into the GAC layer. Accordingly, the obligate or facultative anaerobic bacteria present in the GAC layer were relatively lower compared to those without internal recirculation (e.g., only 1.5-2.5% of Clostridia with recirculation *vs.* 20.8% of Clostridia, 6.7% of *Anaeroplasma*, 1.5% of *Lactobacillus*, 1.2% of *Bacterioides* without recirculation).

4. Conclusions

In this study, the effects of internal recirculation and membrane packing density on the reactor performance of the biocarriers facilitated GDM systems were studied. The presence of internal

418 recirculation could effectively improve the permeate water quality and membrane performance.
419 In addition, in the presence of internal recirculation, the low membrane packing density with
420 the longer HRT and higher recirculation ratio could result in higher nitrogen removal ratios,
421 enhanced membrane permeability, and reduced wastewater treatment cost. While, the
422 membrane packing density did not significantly affect DOC removal efficiency and microbial
423 community compositions.

424 **Acknowledgements**

425 The Economic Development Board (EDB) of Singapore is acknowledged for funding the
426 Singapore Membrane Technology Centre (SMTC), Nanyang Technological University. The
427 authors express their gratitude to Prof. Eberhard Morgenroth at Institute of Environmental
428 Engineering of ETH Zürich (Switzerland) for his advice and support.

429

References

Alleman, J. (1985) Elevated nitrite occurrence in biological wastewater treatment systems. Water science and technology 17(2-3), 409-419.

Braak, E., Alliet, M., Schetrite, S. and Albasi, C. (2011) Aeration and hydrodynamics in submerged membrane bioreactors. Journal of Membrane Science 379(1), 1-18.

Broeckmann, A., Busch, J., Wintgens, T. and Marquardt, W. (2006) Modeling of pore blocking and cake layer formation in membrane filtration for wastewater treatment. Desalination 189(1), 97-109.

Caporaso, J.G., Kuczynski, J., Stombaugh, J., Bittinger, K., Bushman, F.D., Costello, E.K., Fierer, N., Peña, A.G., Goodrich, J.K., Gordon, J.I., Huttley, G.A., Kelley, S.T., Knights, D., Koenig, J.E., Ley, R.E., Lozupone, C.A., McDonald, D., Muegge, B.D., Pirrung, M., Reeder, J., Sevinsky, J.R., Turnbaugh, P.J., Walters, W.A., Widmann, J., Yatsunenko, T., Zaneveld, J. and Knight, R. (2010) QIIME allows analysis of high-throughput community sequencing data. Nature Methods 7(5), 335-336.

Characklis, W.G. (1981) Bioengineering report: fouling biofilm development: a process analysis. Biotechnology and Bioengineering 23(9), 1923-1960.

Deng, L., Guo, W., Ngo, H.H., Zhang, X., Wang, X.C., Zhang, Q. and Chen, R. (2016) New functional biocarriers for enhancing the performance of a hybrid moving bed biofilm reactor–membrane bioreactor system. Bioresource technology 208, 87-93.

Derlon, N., Koch, N., Eugster, B., Posch, T., Pernthaler, J., Pronk, W. and Morgenroth, E. (2013) Activity of metazoa governs biofilm structure formation and enhances permeate flux during Gravity-Driven Membrane (GDM) filtration. Water Research 47(6), 2085-2095.

Ding, A., Liang, H., Li, G., Derlon, N., Szivak, I., Morgenroth, E. and Pronk, W. (2016) Impact of aeration shear stress on permeate flux and fouling layer properties in a low pressure membrane bioreactor for the treatment of grey water. Journal of Membrane Science 510, 382-390.

Ding, A., Wang, J., Lin, D., Tang, X., Cheng, X., Li, G., Ren, N. and Liang, H. (2017) In situ coagulation versus pre-coagulation for gravity-driven membrane bioreactor during decentralized sewage treatment: Permeability stabilization, fouling layer formation and biological activity. Water Research 126, 197-207.

Escobar, I.C. and Randall, A.A. (2001) Assimilable organic carbon (AOC) and biodegradable dissolved organic carbon (BDOC):: complementary measurements. Water Research 35(18), 4444-4454.

Huber, S.A., Balz, A., Abert, M. and Pronk, W. (2011) Characterisation of aquatic humic and non-humic matter with size-exclusion chromatography – organic carbon detection – organic nitrogen detection (LC-OCD-OND). Water Research 45(2), 879-885.

Jabornig, S. and Podmirseg, S.M. (2015) A novel fixed fibre biofilm membrane process for on- site greywater reclamation requiring no fouling control. Biotechnology and bioengineering 112(3), 484-493.

Judd, S. (2010) The MBR book: principles and applications of membrane bioreactors for water and wastewater treatment, Elsevier.

Klein, T., Zihlmann, D., Derlon, N., Isaacson, C., Szivak, I., Weissbrodt, D.G. and Pronk, W. (2016) Biological control of biofilms on membranes by metazoans. Water Research 88, 20-29.

Künzle, R., Pronk, W., Morgenroth, E. and Larsen, T.A. (2015) An energy-efficient membrane bioreactor for on-site treatment and recovery of wastewater. Journal of Water, Sanitation and Hygiene for Development 5(3), 448-455.

Lee, S., Sutter, M., Burkhardt, M., Wu, B. and Chong, T.H. (2019) Biocarriers facilitated gravity-driven membrane (GDM) reactor for wastewater reclamation: Effect of intermittent aeration cycle. Science of the Total Environment 694, 133719.

Maere, T., Verrecht, B., Moerenhout, S., Judd, S. and Nopens, I. (2011) BSM-MBR: A benchmark simulation model to compare control and operational strategies for membrane bioreactors. Water Research 45(6), 2181-2190.

Nguyen, A.V., Pham, N.T., Nguyen, T.H., Morel, A. and Tonderski, K. (2007) Improved septic tank with constructed wetland, a promising decentralized wastewater treatment alternative in Vietnam.

Nguyen, T.V., Jeong, S., Pham, T.T.N., Kandasamy, J. and Vigneswaran, S. (2014) Effect of granular activated carbon filter on the subsequent flocculation in seawater treatment. Desalination 354, 9-16.

Peinemann, K.-V. and Nunes, S.P. (2010) Membranes for water treatment, John Wiley & Sons.

501 Peter-Varbanets, M., Hammes, F., Vital, M. and Pronk, W. (2010) Stabilization of flux during dead-
502 end ultra-low pressure ultrafiltration. Water Research 44(12), 3607-3616.
503
504 Pramanik, B.K., Roddick, F.A., Fan, L., Jeong, S. and Vigneswaran, S. (2015) Assessment of biological
505 activated carbon treatment to control membrane fouling in reverse osmosis of secondary effluent for
506 reuse in irrigation. Desalination 364, 90-95.
507
508 Pronk, W., Ding, A., Morgenroth, E., Derlon, N., Desmond, P., Burkhardt, M., Wu, B. and Fane, A.G.
509 (2019) Gravity-driven membrane filtration for water and wastewater treatment: A review. Water
510 research 149, 553-565.
511
512 Rhee, S.-K., Lee, J.J. and Lee, S.-T. (1997) Nitrite accumulation in a sequencing batch reactor during
513 the aerobic phase of biological nitrogen removal. Biotechnology Letters 19(2), 195-198.
514
515 Seidel, A. and Elimelech, M. (2002) Coupling between chemical and physical interactions in natural
516 organic matter (NOM) fouling of nanofiltration membranes: implications for fouling control. Journal
517 of Membrane Science 203(1), 245-255.
518
519 Tang, X., Pronk, W., Ding, A., Cheng, X., Wang, J., Xie, B., Li, G. and Liang, H. (2018) Coupling
520 GAC to ultra-low-pressure filtration to modify the biofouling layer and bio-community: flux
521 enhancement and water quality improvement. Chemical Engineering Journal 333, 289-299.
522
523 Verrecht, B., Maere, T., Nopens, I., Brepols, C. and Judd, S. (2010) The cost of a large-scale hollow
524 fibre MBR. Water Research 44(18), 5274-5283.
525
526 Wang, Y., Fortunato, L., Jeong, S. and Leiknes, T. (2017) Gravity-driven membrane system for
527 secondary wastewater effluent treatment: Filtration performance and fouling characterization.
528 Separation and Purification Technology 184, 26-33.
529
530 Wu, B., Christen, T., Tan, H.S., Hochstrasser, F., Suwarno, S.R., Liu, X., Chong, T.H., Burkhardt, M.,
531 Pronk, W. and Fane, A.G. (2017) Improved performance of gravity-driven membrane filtration for
532 seawater pretreatment: Implications of membrane module configuration. Water Research 114, 59-68.
533
534 Wu, B., Soon, G.Q.Y. and Chong, T.H. (2019) Recycling rainwater by submerged gravity-driven
535 membrane (GDM) reactors: Effect of hydraulic retention time and periodic backwash. Science of the
536 Total Environment 654, 10-18.

537

Table 1. Operating conditions of the biocarriers facilitated GDM reactors.

	R1-HP	R2-LP
pH	7.3±0.4	7.2±0.2
DO (mg/L)	3.4±0.7	3.8±0.9
Effective total membrane area (cm^2)	536	138
Membrane packing density (m^2/m^3)	1150	290
Averaged HRT[a] (h)	~59	~154
Averaged recirculation ratio[b]	~3.5	~9.2

[a] HRT was determined daily and averaged HRT was calculated by averaging the daily HRT.
[b] The recirculation ratio was defined as the ratio of recirculation flow rate (0.52 L/h) to the feed flow rate. Averaged recirculation ratio was calculated by averaging the daily recirculation ratio.

Table 2. The energy consumption and wastewater treatment cost of R1-HP and R2-LP.

		R1-HP	R2-LP
Permeate water productivity (m^3/d)		0.223	0.081
Energy consumption (kWh/m^3)	Feed pump	0.003	0.003
	Recirculation pump	0.010	0.027
	Aeration	0.020	0.056
	Total	0.034	0.087
Capital cost (Euro/m^3)	Membranes[a]	0.182	0.127
	Biocarriers (GAC)[b]	0.003	0.007
	Recirculation pump[c,d]	0.0006	0.0016
	Others[c] (feed pump[d], blower, and reactor construction)	0.003	0.008
	Total	0.189	0.144
Operating cost (Euro/m^3)	Energy[e]	0.003	0.009
Total cost (Euro/m^3)		0.192	0.153

[a] Membrane cost and lifespan was assumed to be 50 Euro/m^2 and 10 years, respectively (Judd 2010).

[b] GAC cost and lifespan was estimated as 972 Euro/ton and 5 years, respectively (Nguyen et al. 2014).

[c] (Verrecht et al. 2010)

[d] The capacity of feed pump and recirculation pump was assumed to be the same as 40 L/h for both reactors.

[e] Electricity cost was assumed to be 0.1 Euro/kWh.

Table 3. A comparison of permeate water quality and flux in presence and absence of internal recirculation in the biocarriers facilitated GDM reactors.

		Without internal recirculation (Lee et al. 2019)[a]	With internal recirculation	
			R1-HP	R2-LP[a]
Feed	DOC (mg/L)	24.2±7.5	42.3±6.8	
	TN (mg/L)	36.8±4.0	40.0±4.3	
In the reactor	DOC (mg/L) (Removal)	4.4±0.8 (80.6%)	4.7±0.9 (88.5%)	3.6±0.7 (91.4%)
	Ammonia (mg/L) (Removal)	5.3±1.9 (84.7%)	1.2±0.5 (96.9%)	0.8±0.2 (97.9%)
	TN (mg/L) (Removal)	25.6±3.1 (30.3%)	14.3±2.4 (63.8%)	8.5±0.9 (78.6%)
Permeate	DOC (mg/L) (Removal)	3.0±1.8 (85.0%)	2.3±0.9 (94.5%)	3.0±1.4 (92.8%)
	TN (mg/L) (Removal)	25.1±2.3 (31.5%)	13.8±2.7 (65.1%)	7.9±0.9 (79.8%)
Stabilized flux (LMH)		~2.0	~3.1	~4.5
Cake layer resistance (m^{-1})		4.02×10^{12}	1.72×10^{11}	0.94×10^{11}

[a] In both reactors, the membrane module had the same packing density.

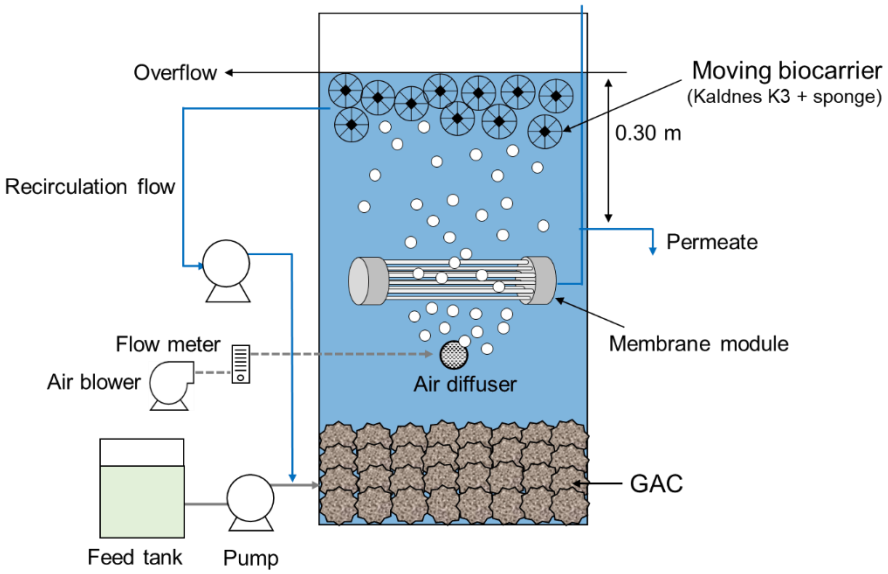

Figure 1. A schematic diagram of the biocarriers facilitated GDM reactor.

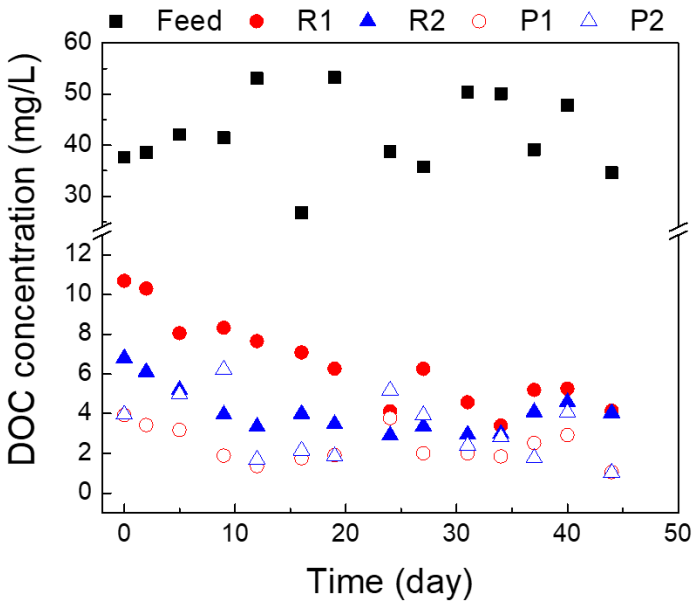

Figure 2. DOC concentrations in the feed, reactor, permeate of R1-HP and R2-LP. R and P represent reactor and permeate, respectively.

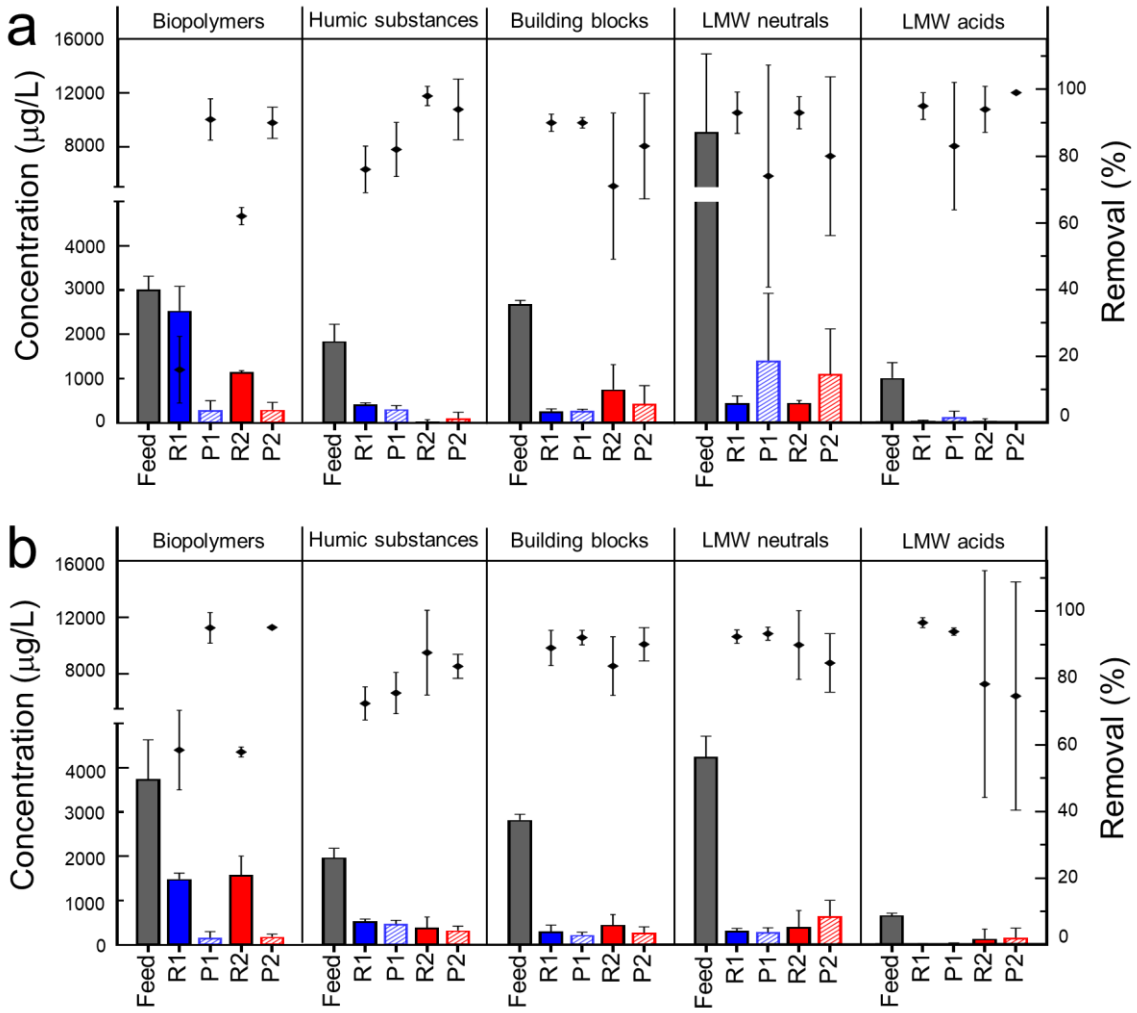

Figure 3. Soluble organic fractions in the feed, reactor, and permeate of R1-HP and R2-LP. (a) during initial stage (Day 0-20, n=2), and (b) during stable stage (Day 21-45, n=3). Columns indicate the concentrations while dots indicate the removal efficiency calculated based on the data in the feed. R and P represent reactor and permeate, respectively.

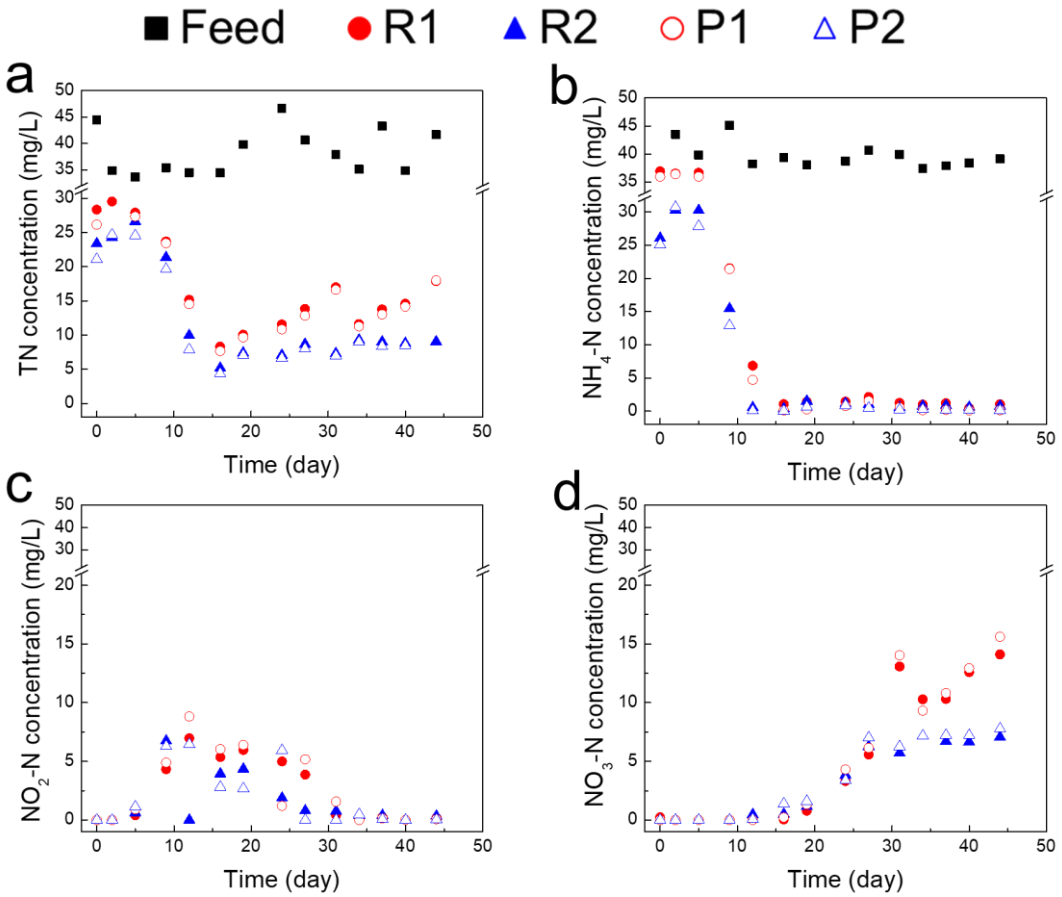

Figure 4. Nitrogen concentrations in the feed, reactor, permeate of R1-HP and R2-LP. (a) TN, (b) Ammonia, (c) Nitrite, (d) Nitrate. R and P represent reactor and permeate, respectively.

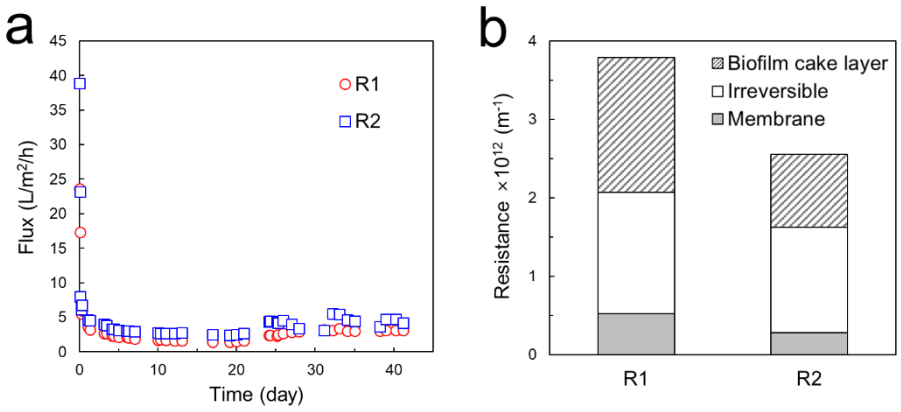

Figure 5. Membrane performances of R1-HP and R2-LP. (a) Permeate flux. (b) Resistance distribution.

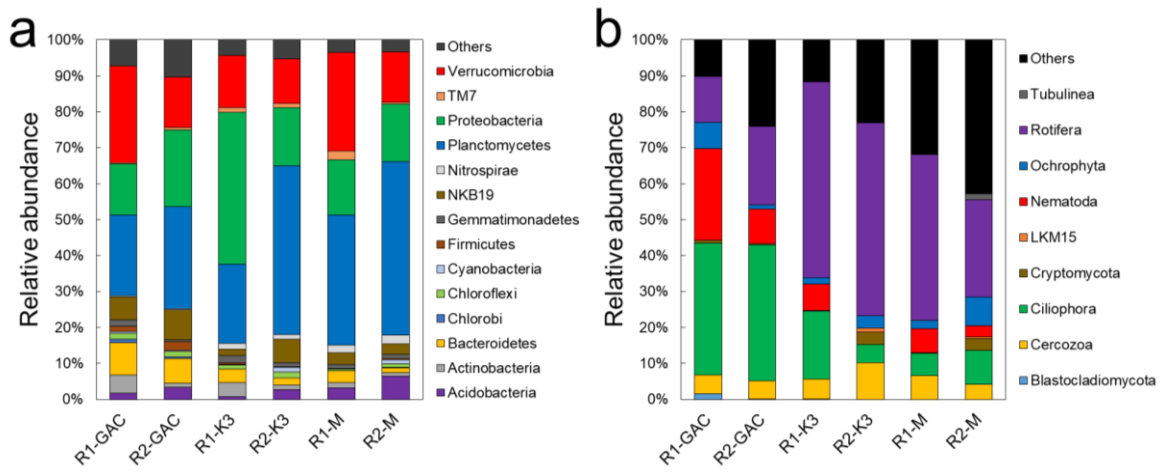

Figure 6. Compositions of prokaryotic (a) and eukaryotic (b) communities in R1-HP and R2-LP. K3 and M represent moving biocarrier (Kaldnes K3 with sponge) and membrane sample, respectively.

CRediT author statement

Lee Seonki: Conceptualization, Investigation, Writing - Original Draft, Visualization, Review & Editing

Guillaume Olivier Badoux: Conceptualization, Methodology, Validation

Wu Bing: Conceptualization, Methodology, Writing - Review & Editing, Supervision

Chong Tzyy Haur: Conceptualization, Writing - Review & Editing, Supervision

Declaration of Interest Statement